Circulation
JOURNAL OF THE AMERICAN HEART ASSOCIATION

Rheb is a Critical Regulator of Autophagy During Myocardial Ischemia : Pathophysiological Implications in Obesity and Metabolic Syndrome

Sebastiano Sciarretta, Peiyong Zhai, Dan Shao, Yasuhiro Maejima, Jeffrey Robbins, Massimo Volpe, Gianluigi Condorelli and Junichi Sadoshima

Circulation 2012, 125:1134-1146: originally published online January 31, 2012
doi: 10.1161/CIRCULATIONAHA.111.078212
Circulation is published by the American Heart Association. 7272 Greenville Avenue, Dallas, TX 72514
 Print ISSN: 0009-7322. Online ISSN: 1524-4539

Rheb is a Critical Regulator of Autophagy During Myocardial Ischemia

Pathophysiological Implications in Obesity and Metabolic Syndrome

Sebastiano Sciarretta, MD; Peiyong Zhai, MD, PhD; Dan Shao, BS; Yasuhiro Maejima, MD, PhD; Jeffrey Robbins, PhD; Massimo Volpe, MD; Gianluigi Condorelli, MD, PhD; Junichi Sadoshima, MD, PhD

Background—Rheb is a GTP-binding protein that promotes cell survival and mediates the cellular response to energy deprivation (ED). The role of Rheb in the regulation of cell survival during ED has not been investigated in the heart.

Methods and Results—Rheb is inactivated during cardiomyocyte (CM) glucose deprivation (GD) in vitro, and during acute myocardial ischemia in vivo. Rheb inhibition causes mTORC1 inhibition, because forced activation of Rheb, through Rheb overexpression in vitro and through inducible cardiac-specific Rheb overexpression in vivo, restored mTORC1 activity. Restoration of mTORC1 activity reduced CM survival during GD and increased infarct size after ischemia, both of which were accompanied by inhibition of autophagy, whereas Rheb knockdown increased autophagy and CM survival. Rheb inhibits autophagy mostly through Atg7 depletion. Restoration of autophagy, through Atg7 reexpression and inhibition of mTORC1, increased cellular ATP content and reduced endoplasmic reticulum stress, thereby reducing CM death induced by Rheb activation. Mice with high-fat diet–induced obesity and metabolic syndrome (HFD mice) exhibited deregulated cardiac activation of Rheb and mTORC1, particularly during ischemia. HFD mice presented inhibition of cardiac autophagy and displayed increased ischemic injury. Pharmacological and genetic inhibition of mTORC1 restored autophagy and abrogated the increase in infarct size observed in HFD mice, but they failed to protect HFD mice in the presence of genetic disruption of autophagy.

Conclusions—Inactivation of Rheb protects CMs during ED through activation of autophagy. Rheb and mTORC1 may represent therapeutic targets to reduce myocardial damage during ischemia, particularly in obese patients. **(*Circulation*. 2012;125:1134-1146.)**

Key Words: apoptosis ■ ischemia ■ obesity ■ signal transduction

Heart failure is viewed as one of the major healthcare problems worldwide, with acute myocardial infarction (MI) as the most common predisposing cause.[1] It is fundamental to clarify the mechanisms regulating cardiomyocyte (CM) death and survival during ischemic injury to find new therapies to reduce the amount of myocardial loss after a sudden coronary occlusion.

Clinical Perspective on p 1146

Ras homology enriched in brain (Rheb) is a small GTP-binding protein that has been shown to regulate the cellular stress response, both in lower organisms and in mammalian cell lines. In particular, Rheb appears to be a critical sensor of energy stress, being inactivated under this condition. Inhibition of Rheb during cellular stress promotes the upregulation of adaptive mechanisms, such as cell cycle arrest and growth inhibition, which may save energy, favor DNA repair, and thus be protective.[2–4] On the contrary, Rheb is hyperactivated in cancer cells, where it promotes stress resistance and survival, and Rheb activation was found to directly inhibit apoptotic pathways induced by amino acid deprivation and genotoxic stress.[5,6] Therefore, it is not clear whether Rheb activity is protective or detrimental during cellular stress. Remarkably, the role of Rheb in response to acute energy deprivation, and in regulation of cell death and survival, has never been investigated in the heart.

Rheb activity is regulated by upstream kinases, such as Akt, AMP-activated protein kinase (AMPK), and glycogen

Received August 15, 2011; accepted January 23, 2012.

From the Cardiovascular Research Institute, Department of Cell Biology and Molecular Medicine, University of Medicine and Dentistry of New Jersey, New Jersey Medical School, Newark, NJ (S.S., P.Z., D.S., Y.M., J.S.); IRCCS Neuromed, Pozzilli (IS), Italy (S.S., M.V.); Molecular Cardiovascular Biology, Heart Institute, Cincinnati Children's Hospital, Cincinnati, OH (J.R.); Cardiology Department, IInd School of Medicine, University of Rome "Sapienza," S. Andrea Hospital, Rome, Italy (M.V.); and Department of Medicine, University of California San Diego, La Jolla, CA (G.C.).

The online-only Data Supplement is available with this article at http://circ.ahajournals.org/lookup/suppl/doi:10.1161/CIRCULATIONAHA.111.078212/-/DC1.

Correspondence to Junichi Sadoshima, MD, Cardiovascular Research Institute, University of Medicine and Dentistry of New Jersey, New Jersey Medical School, 185 South Orange Ave, Medical Science Building G-609, Newark, NJ 07103. E-mail Sadoshju@umdnj.edu

Circulation **is available at http://circ.ahajournals.org** **DOI: 10.1161/CIRCULATIONAHA.111.078212**

synthase kinase-3β, which control Rheb through direct modulation of the heterodimer composed of the tuberous sclerosis complex proteins 1 (TSC1) and 2 (TSC2). The TSC1/TSC2 complex inhibits Rheb by exerting a strong GTPase activity toward it.[2,7] Rheb directly binds and selectively activates the multiprotein complex 1 of mammalian target of rapamycin (mTORC1), which in turn mediates many cellular functions, such as protein translation.[8] mTORC1 is also inhibited in response to energy stress, and its inactivation reduces protein synthesis and upregulates autophagy.[8] However, mTORC1 activation also promotes cell survival and inhibits apoptosis in several stress conditions, and, therefore, whether mTORC1 inhibition is detrimental or protective during cellular stress is stimulus dependent.[5,8]

The role of mTORC1 in mediating survival and death of CMs has only been investigated in models of chronic cardiac remodeling, with discordant results.[9–11] Importantly, the effect of direct and selective mTORC1 versus mTORC2 modulation during CM acute energy deprivation, such as myocardial ischemia, remains to be elucidated. It is also unclear how mTORC1 is modulated during CM energy deprivation and whether Rheb, an immediate upstream regulator of mTORC1, is critically involved in such regulation in CMs.

In our study, we investigated the role of Rheb in the regulation of cell death and survival during CM starvation and ischemia, and the underlying molecular mechanisms. In particular, we studied whether a direct and selective modulation of mTORC1 induced by Rheb is involved in the effects exerted by Rheb on CM survival during energy stress. Recent reports have shown that obesity and metabolic syndrome, which are characterized by an increased risk of cardiovascular mortality[12] and increased myocardial susceptibility to ischemic injury,[13–16] are associated with a hyperactivation of tissue mTORC1.[17,18] Therefore, we also evaluated whether cardiac mTORC1 is activated in obesity and metabolic syndrome, whether Rheb is involved in such phenomena, and whether a deregulated activation of Rheb and mTORC1 may be responsible for the increased susceptibility to ischemia associated with these conditions.

Methods

Experimental Procedures

Experimental procedures and animal models are described in the expanded Methods section in the online-only Data Supplement. Experimental procedures, heterozygous GFP-LC3 transgenic mice, *beclin-1* knockout mice, and conditional *mTOR* knockout mice have also been described elsewhere.[9,19,20] All experimental procedures with animals were approved by the Institutional Animal Care and Use Committee of the University of Medicine and Dentistry of New Jersey.

Statistics

Data are expressed as mean±SEM. When specified in the figure legends, presentation of bar charts was standardized by control mean×100, so that the presented bars represent the mean percentage of variation±SEM, with respect to the control mean. The difference in means between 2 groups was evaluated using the *t* test when sample size was appropriate and the population was normally distributed; otherwise, the Mann-Whitney *U* test was adopted. When differences among 3 or more groups were evaluated, the one-way analysis of variance or the Kruskal-Wallis test was used. The post hoc comparisons were performed by use of the Bonferroni post hoc test or the Mann-Whitney *U* test with Bonferroni correction. The shown statistical significance of differences between groups was always calculated by post hoc comparisons when multiple groups were compared. Statistical analyses were performed with the use of SPSS 15.0 (SPSS Inc, Chicago, IL) and GraphPad-Prism 5.00 (GraphPad-Software, San Diego, CA). Probability values of <0.05 were considered statistically significant.

Results

Rheb Mediates mTORC1 Inhibition During Starvation in CMs

To investigate whether Rheb acts as a sensor of energy deprivation in CMs, neonatal rat ventricular CMs were subjected to glucose deprivation (GD). GTP binding of Rheb was decreased significantly in response to GD (Figure 1A), indicating that Rheb is inactivated by GD. During GD, phosphorylation of $p70^{S6K}$ and 4E-BP1 was progressively reduced, indicating that mTORC1 was inhibited (Figure 1B). Knockdown of Rheb, with adenovirus harboring shRNA-Rheb, inhibited phosphorylation of $p70^{S6K}$ at baseline, suggesting that inactivation of Rheb is sufficient to inactivate mTORC1 (online-only Data Supplement Figure IA). Transduction of CMs with adenovirus harboring wild-type Rheb abolished the GD-induced decreases in phosphorylation of $p70^{S6K}$ and 4E-BP1 (Figure 1C through 1E and online-only Data Supplement Figure IB), suggesting that Rheb inactivation is required for GD-induced suppression of mTORC1. In addition, Rheb physically interacts with mTOR both at baseline and during GD (online-only Data Supplement Figure IC), thus indicating that Rheb directly regulates mTORC1 in CMs.

Rheb is negatively regulated by the GTPase-activating protein activity of the TSC1/TSC2 complex.[7] Downregulation of TSC2, with adenovirus harboring shRNA-TSC2 (online-only Data Supplement Figure ID), induced phosphorylation of $p70^{S6K}$, suggesting that endogenous TSC2 negatively regulates mTORC1 in CMs (online-only Data Supplement Figure IE and IF). Activation of mTORC1 by downregulation of TSC2 was abolished in the presence of Rheb knockdown, suggesting that TSC2 regulates mTORC1 through Rheb (online-only Data Supplement Figure IE and IF). On the other hand, as indicated by the phosphorylation status of Akt, the activity of mTORC2, another branch of the mTOR pathway, was unaffected by GD, and overexpression of Rheb failed to activate Akt (online-only Data Supplement Figure IG and IH). These results suggest that GD inhibits mTORC1, but not mTORC2, by inactivating Rheb.

Activation of Rheb Sensitizes CMs to Cell Death During GD, Whereas Inhibition Is Protective

We then investigated the role of Rheb in regulating CM survival during GD. Although Rheb is cell protective in other cell types, CMs in which the activity of mTORC1 was normalized with overexpressed Rheb displayed decreased survival after 10 and 18 hours of GD in comparison with control virus–treated CMs (Figure 2A). CMs overexpressed with Rheb displayed significantly more apoptosis and necrosis, as assessed by TdT-mediated dUTP nick-end labeling (TUNEL) assays and propidium iodide staining, respectively

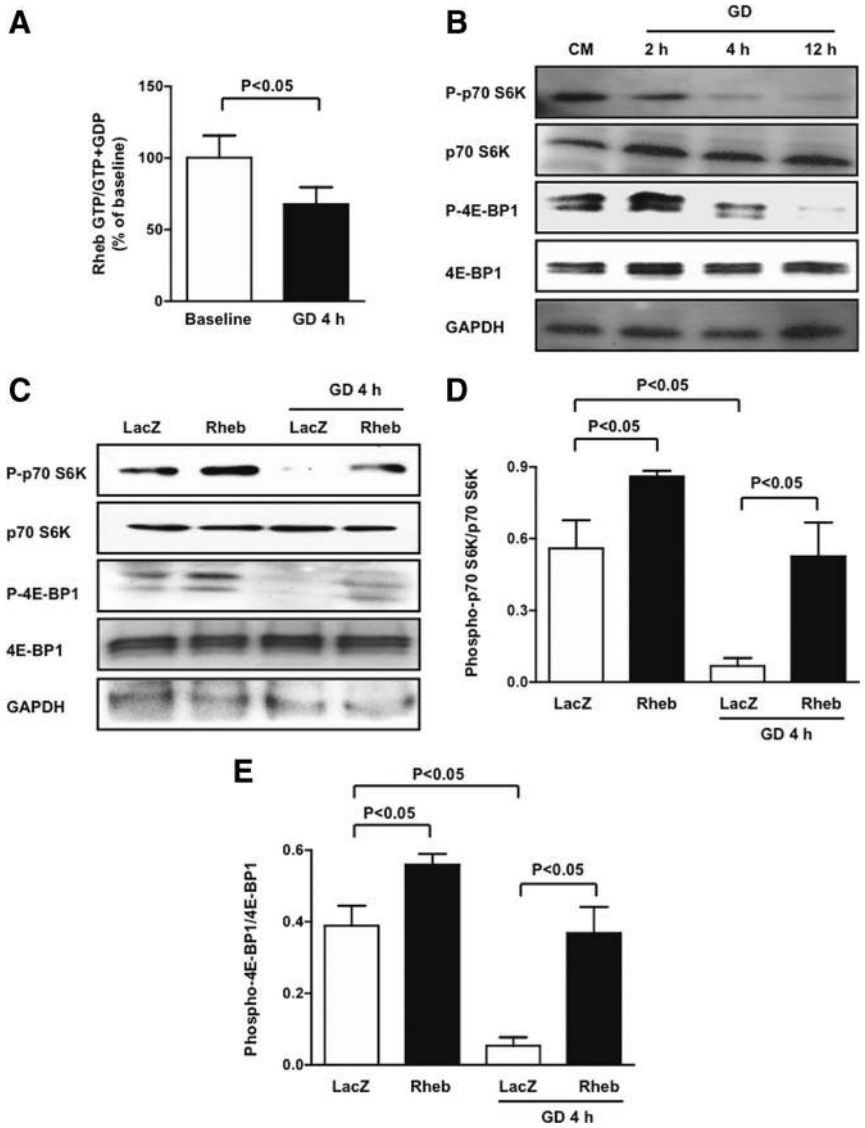

Figure 1. mTORC1 is downregulated during GD through Rheb inactivation. **A**, Rheb activity was assessed by the ratio of Rheb-bound GTP to Rheb-bound GTP+GDP levels at baseline and during GD; n=5. **B**, CMs were subjected to GD for different periods of time. Phosphorylation statuses of $p70^{S6K}$ (Thr 389) and 4E-BP1 (Thr 37/46) were evaluated. **C** through **E**, CMs were transduced with adenovirus harboring wild-type Rheb or LacZ. After 48 hours, phosphorylation statuses of $p70^{S6K}$ and 4E-BP1 were evaluated at baseline and after GD. Immunoblots and densitometric analyses are presented. n=5. GD indicates glucose deprivation; CM, cardiomyocyte.

(Figure 2B and 2C, online-only Data Supplement Figure IIA). TSC2 knockdown also decreased survival and increased apoptosis of CMs in response to GD (Figure 2D and online-only Data Supplement Figure IIB). Conversely, downregulation of endogenous Rheb increased the survival of CMs during GD and rescued the decrease in cell survival in the presence of TSC2 knockdown during GD (Figure 2E). Furthermore, selective inhibition of mTORC1, through Raptor downregulation, with adenovirus harboring shRNA-Raptor, significantly increased CM survival during GD in Rheb-overexpressing CMs. In contrast, selective mTORC2 inhibition, through Rictor depletion, did not increase survival in Rheb-overexpressing CMs during GD (Figure 2F). Collectively, these data suggest that Rheb negatively regulates CM survival during GD through mTORC1 activation. Thus, inactivation of endogenous Rheb during GD is an adaptive mechanism that promotes survival of CMs.

Rheb Regulates CM Autophagy

We investigated the molecular mechanism through which inactivation of Rheb protects CMs during GD. Because Rheb inactivation causes mTORC1 inhibition during GD, and because mTOR is a negative regulator of autophagy,[21] we hypothesized that downregulation of Rheb during GD is required for stimulation of autophagy, which may be protective in this context.[19] As shown previously, GD increased LC3-II and decreased p62, a protein degraded by autophagy,[21] suggesting that GD activates autophagy in CMs. However, in Rheb-overexpressing CMs, LC3-II expression was lower and expression of p62 was greater, both at baseline and during GD (Figure 3A through 3C). The number of GFP-LC3 dots, an indicator of autophagosome accumulation, during GD was significantly smaller in Rheb-overexpressing CMs than in control CMs (Figure 3D and 3E). Rheb overexpression induced significant downregulation of autophagy genes, including *beclin-1*, *ulk-1*, *atg4*, and *atg7* (Figure 3F). Conversely, downregulation of endogenous Rheb significantly increased autophagy at baseline and during GD (online-only Data Supplement Figure III). These results suggest that endogenous Rheb negatively regulates autophagy and that inactivation of Rheb is necessary and sufficient for stimulation of autophagy in CMs during GD.

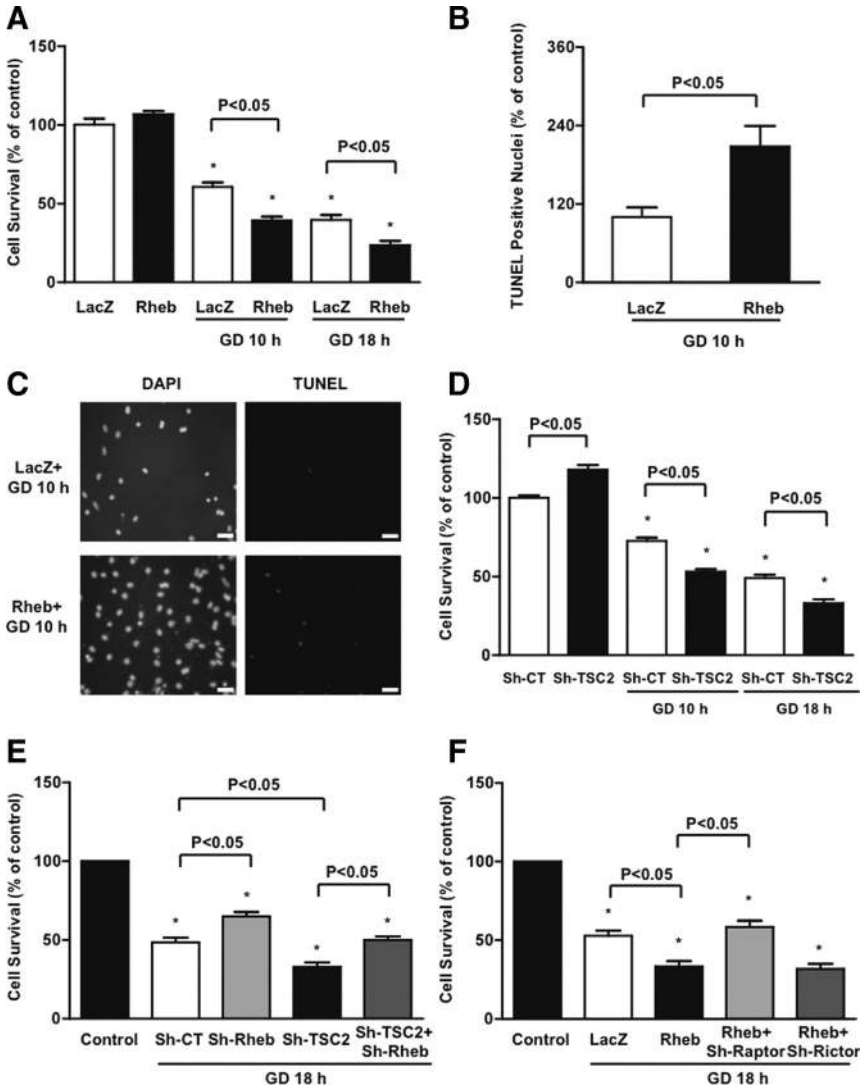

Figure 2. Rheb activation during GD increases CM death and apoptosis. **A**, Cell viability was evaluated in CMs transduced with Ad-Rheb or Ad-LacZ at baseline and during GD. n=4. **B** and **C**, Percentage of TUNEL-positive cells was also evaluated after GD. n=4, bar=50 μm. **D**, CMs were transduced with Ad harboring sh-RNA-TSC2 or with sh-scramble. After 96 hours, cell viability was evaluated at baseline and after GD. n=5. **E**, Cell viability was evaluated in CMs transduced with sh-scramble (sh-CT), sh-Rheb, sh-TSC2, or sh-Rheb plus sh-TSC2 at baseline and after GD. n=5. **F**, Cell viability was evaluated in CMs transduced with Ad-LacZ, Ad-Rheb, or Ad-Rheb plus sh-Raptor or sh-Rictor, at baseline and after GD. n=3. Cell viability was assessed by Cell Titer Blue assay. Data are presented as a percentage of the relevant control (regular medium), with the control being set at 100%. *$P<0.05$ with respect to relevant control (regular medium). Ad indicates adenovirus; sh, short hairpin; GD, glucose deprivation; CM, cardiomyocyte; DAPI, 4,6-diamidino-2-phenylindole-2-HCl; TUNEL, TdT-mediated dUTP nick-end labeling.

We then asked if autophagy mediates the cell-protective effect of Rheb inactivation. The protective effect of Rheb downregulation during GD was completely abrogated when Beclin-1 was downregulated with adenovirus harboring shRNA-*beclin1* (Figure 3G). These results suggest that autophagy plays an important role in mediating the protective effect of Rheb inactivation during GD. Conversely, to restore autophagy during GD in Rheb-overexpressing CMs, we expressed Atg7 with adenovirus transduction (online-only Data Supplement Figure IVA). We took this approach because Atg7 is a crucial protein for autophagosome formation, because Atg7 is markedly downregulated in Rheb-overexpressing CMs, and because overexpression of Atg7 is sufficient to reinduce autophagy when autophagy is inhibited.[21,22] Atg7 overexpression significantly restored autophagy in Rheb-overexpressing CMs during GD (online-only Data Supplement Figure IVB through IVD). We also used trehalose, which induces autophagy without affecting the mTORC1 pathway.[23] Trehalose restored Atg7 and Beclin-1 expression in Rheb-overexpressing CMs without affecting the mTORC1 pathway, thereby restoring autophagy during GD (online-only Data Supplement Figure IVE and IVF). Importantly, both Atg7 expression and trehalose pretreatment significantly increased the survival of Rheb-overexpressing CMs during GD (Figure 3H). Collectively, these results suggest that Rheb regulates the survival and death of CMs during GD through regulation of autophagy in vitro.

Rheb Overexpression Increases Energy Stress and Endoplasmic Reticulum Stress During GD

Important consequences of autophagy include restoration of ATP contents and protein quality control. Rheb overexpression during GD significantly enhanced ATP depletion, whereas Rheb disruption significantly increased ATP content (Figure 4A). Overexpression of Rheb increased GRP78, phosphorylation of protein kinase RNA-like endoplasmic reticulum kinase and upregulation of Ccaat-enhancer-binding protein homologous protein (CHOP), and Caspase-12 (fragment), markers of endoplasmic reticulum (ER) stress, in CMs during GD (Figure 4B and 4C). Conversely, upregulation of the ER stress markers during GD was significantly attenuated in CMs in which Rheb was knocked down (Figure 4B and 4C). Restoration of autophagy in Rheb-overexpressing CMs,

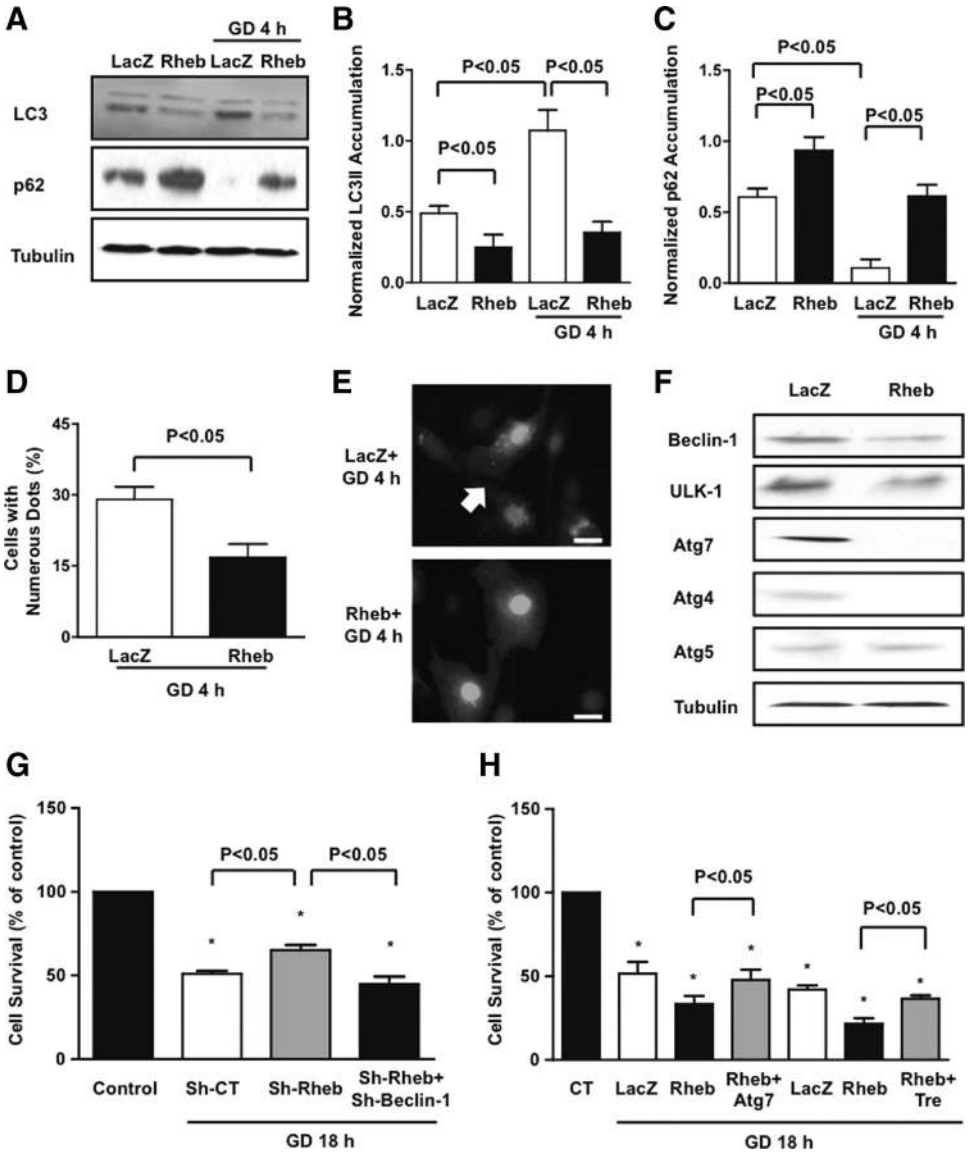

Figure 3. Rheb is a negative regulator of autophagy. **A** through **C**, CMs were transduced with Ad-LacZ or Ad-Rheb for 48 hours. LC3 isoforms and p62 accumulation were evaluated at baseline or after 4 hours of GD. A representative immunoblot is shown (**A**), together with densitometric analyses of LC3-II (**B**) and p62 (**C**). n=5. **D** and **E**, CMs were transduced with Ad-GFP-LC3 together with Ad-LacZ or Ad-Rheb. GFP-LC3 puncta were evaluated after 4 hours of GD (bar=10 μm). n=3. **F**, Expression of autophagic genes was evaluated in CMs transduced with Ad-LacZ or Ad-Rheb. **G**, Cell viability was evaluated in CMs transduced with sh-scramble, sh-Rheb, or with sh-Rheb plus sh-Beclin-1. n=4. Data are presented as a percentage of the relevant CT (baseline), with CT being set at 100%. **H**, Cell viability was evaluated in CMs transduced with Ad-LacZ, Ad-Rheb, and with Ad-Rheb together with Ad-Atg7 or trehalose. Sucrose treatment (100 mmol/L) was used as control treatment for trehalose. n=3. Atg7=Ad-Atg7. Tre indicates trehalose; Ad, adenovirus; sh, short hairpin; GD, glucose deprivation; CM, cardiomyocyte; CT, control. *$P<0.05$ with respect to cells cultured with a normal medium.

through Atg7 overexpression, significantly attenuated ATP depletion (Figure 4D) and ER stress during GD, indicating that autophagy inhibition is responsible for these derangements (Figure 4E and 4F).

Inhibition of Rheb Is Protective During Prolonged Myocardial Ischemia

To investigate the role of Rheb in regulating CM survival and death in response to energy deprivation in vivo, we used a mouse model of prolonged ischemia, in which the left descending coronary artery was ligated for 3 hours. During ischemia, the GTP-bound form of Rheb was significantly decreased, whereas the total expression of Rheb was not altered, suggesting that Rheb is inactivated by prolonged ischemia in vivo (Figure 5A and 5B). The activity of mTORC1, as evaluated with $p70^{S6K}$ phosphorylation, was also decreased during ischemia (Figure 5C and 5D).

To evaluate the significance of Rheb inhibition during ischemia in vivo, we generated transgenic mice with cardiac-specific overexpression of Rheb (Tg-Rheb) with use of a Tet-off system. In these mice, expression of the Rheb transgene in the heart was induced in the absence of doxycycline. Doxycycline was administered to the mice during the gestational period and for the first 3 to 4 weeks of life to avoid

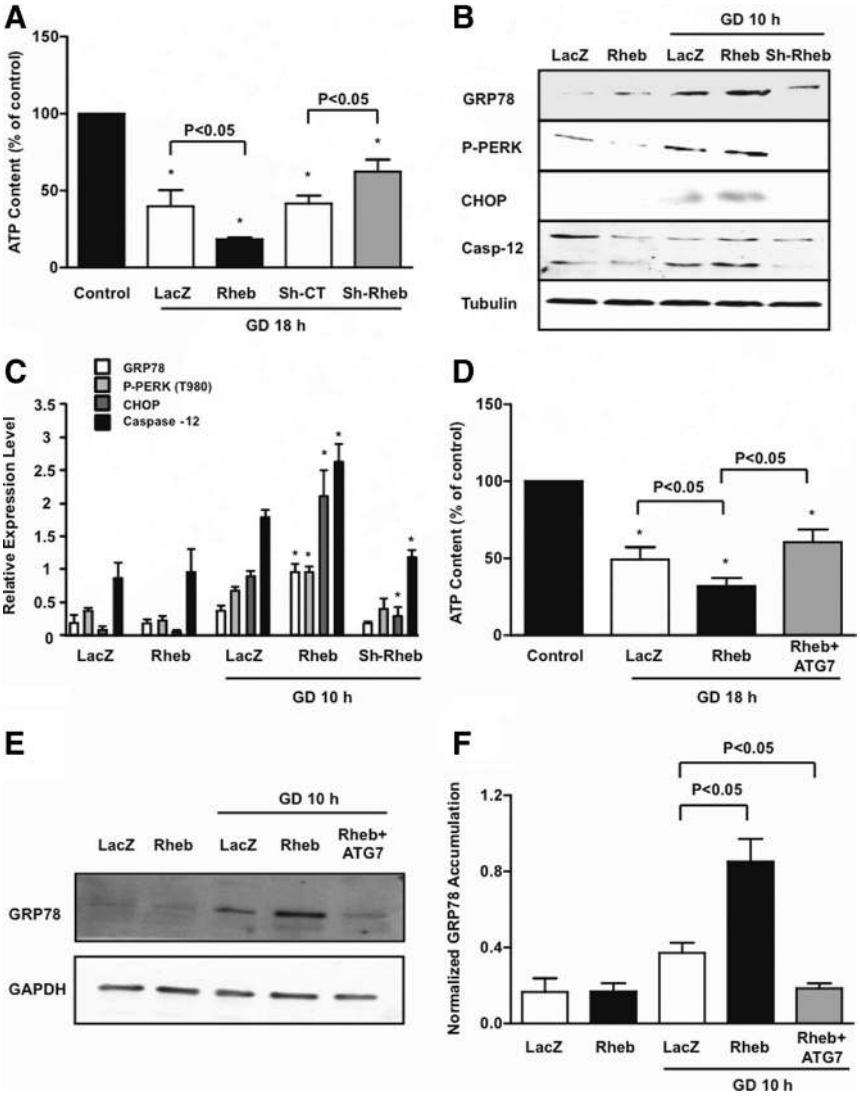

Figure 4. Rheb activation increases ATP depletion and ER stress during GD. **A**, CM ATP content at baseline and after 18 hours of GD was evaluated in CMs with Rheb overexpression or depletion. Data are presented as the fluorescence of each sample as a percentage of the control. **P*<0.05 vs control (regular medium). n=4. **B** and **C**, Unfolded protein response markers were evaluated at baseline and after GD. **P*<0.05 vs LacZ after GD. n=5. **D** through **F**, ATP content (**D**, n=5) and GRP78 accumulation (**E** and **F**, n=3) were evaluated in Rheb-overexpressing CMs with or without Ad-Atg7, after GD. Ad indicates adenovirus; sh, short hairpin; GD, glucose deprivation; CM, cardiomyocyte; CHOP, C/EBP homologous protein.

the effect of transgene expression during cardiac development in Tg-Rheb (Figure 5E and online-only Data Supplement Figure VA and VB). Doxycycline was terminated 6 to 8 weeks before the experiment to allow full transgene expression and eliminate possible actions of doxycycline on cell death/survival. In this protocol, expression of Rheb was 2.3-fold greater in Tg-Rheb than in control littermates (Rheb+/tTA− mice). Rheb exhibited diffuse cytoplasmic distribution in CMs of both control mice and Tg-Rheb (online-only Data Supplement Figure VC and VD). Tg-Rheb presented a normal cardiac phenotype at 3 months of age (online-only Data Supplement Table I). In Tg-Rheb mice, mTORC1 activity was significantly increased, both at baseline and during prolonged ischemia, in comparison with control mice (Figure 5C and 5D), suggesting that Rheb inactivation is required for mTORC1 inhibition during prolonged ischemia. After 3 hours of ischemia, Tg-Rheb mice exhibited a significantly greater MI size than control mice (Figure 5F through 5H**).** The extent of CM apoptosis and necrosis after prolonged ischemia was also greater in Tg-Rheb than in controls, as evaluated with TUNEL and Hairpin-2 staining, respectively (online-only Data Supplement Figure VI). Tg-Rheb presented increased ischemic injury even after a brief period of ischemia (30 minutes), as evaluated with Hairpin-2 staining. Tg-Rheb also exhibited significantly enhanced myocardial damage even after a longer coronary occlusion (6 hours; online-only Data Supplement Figure VII).

There was less induction of autophagy in Tg-Rheb than in control mice at baseline and during ischemia, as indicated by reduced LC3-II and increased p62 accumulation (online-only Data Supplement Figure VIIIA through VIIIC). Expression of p62 did not differ at the mRNA level between controls and Tg-Rheb, indicating that increased p62 accumulation was due to reduced degradation (mRNA expression in Tg-Rheb 0.96-fold versus controls, *P*=NS). The level of myocardial ATP in the ischemic area after ischemia was significantly lower in Tg-Rheb than in controls (online-only Data Supplement Figure VIIID). The level of CHOP, an indicator of ER stress, after ischemia was also significantly greater in Tg-Rheb than in control mice (online-only Data Supplement Figure VIIIE and

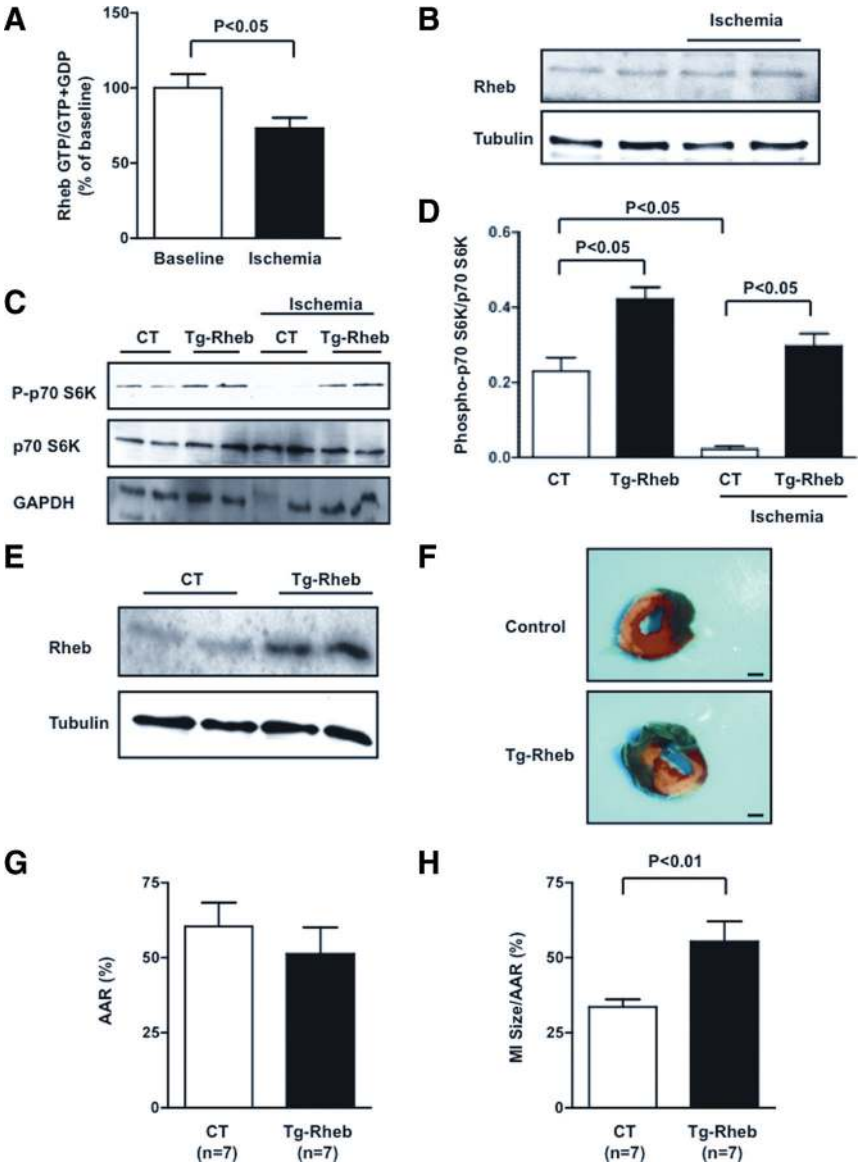

Figure 5. Rheb activation is detrimental during prolonged myocardial ischemia in vivo. **A**, Rheb-bound GTP levels were evaluated at baseline and after 30 minutes of ischemia. n=7. **B**, The amount of Rheb expression was evaluated at baseline and during ischemia. **C** and **D**, Cardiac $p70^{S6K}$ phosphorylation was evaluated in Tg-Rheb mice and controls, both at baseline and after 30 minutes of ischemia. n=4 for each group. **E**, Cardiac Rheb expression was evaluated in Tg-Rheb mice and control mice (FVB background). **F** through **H**, Tg-Rheb and control mice (Rheb+/tTA− and Rheb-/tTA+) were subjected to 3 hours of ischemia. Left ventricular myocardial sections after Alcian blue and triphenyltetrazolium chloride staining is shown (**F**; bar=1 mm), as well as the AAR (**G**) and MI size/AAR (**H**) quantification. AAR indicates area at risk; MI, myocardial infarct; CT, control.

VIIIF). These results indicate that inhibition of endogenous Rheb is protective during prolonged ischemia in vivo.

To evaluate whether the deleterious effect of Rheb overexpression during prolonged ischemia is due to the lack of mTORC1 inactivation and activation of autophagy, rapamycin, a selective inhibitor of mTORC1 and stimulator of autophagy, was administered to Tg-Rheb and control mice just before the prolonged ischemia. Rapamycin inhibited mTORC1 activity and stimulated autophagy in Tg-Rheb mice after prolonged ischemia (Figure 6A). Rapamycin significantly reduced the size of MI in response to prolonged ischemia in Tg-Rheb mice in comparison with vehicle administration (Figure 6B through 6D). Rapamycin treatment also significantly reduced CHOP accumulation and caspase-3 cleavage in Tg-Rheb hearts after prolonged ischemia (Figure 6E and 6F). These results suggest that Rheb promotes myocardial injury during prolonged ischemia by stimulating mTORC1, inhibiting autophagy and stimulating ER stress.

High-Fat Diet–Induced Obesity Is Associated With Deregulation of Rheb and Increased Myocardial Susceptibility to Prolonged Ischemia

Obesity and metabolic syndrome are associated with high cardiovascular mortality and reduced cardiac function after MI.[12–16] Complications of obesity are associated with deregulated mTORC1 activation and inhibition of autophagy in other organs.[17,18,22] We therefore investigated whether obesity is associated with deregulated Rheb activation, which in turn mediates an increased susceptibility to myocardial ischemia.

To induce obesity, C57BL/6J mice were fed with high-fat diet (HFD) mice for 18 to 20 weeks. HFD mice developed obesity and exhibited a significant increase in serum levels of glucose, cholesterol, triglycerides, and nonesterified fatty acid in comparison with mice fed with control diet (CD) mice, suggesting that HFD mice develop metabolic syndrome (online-only Data Supplement Table II). Insulin levels and the HOMA index were significantly elevated in HFD mice, consistent with the notion that these

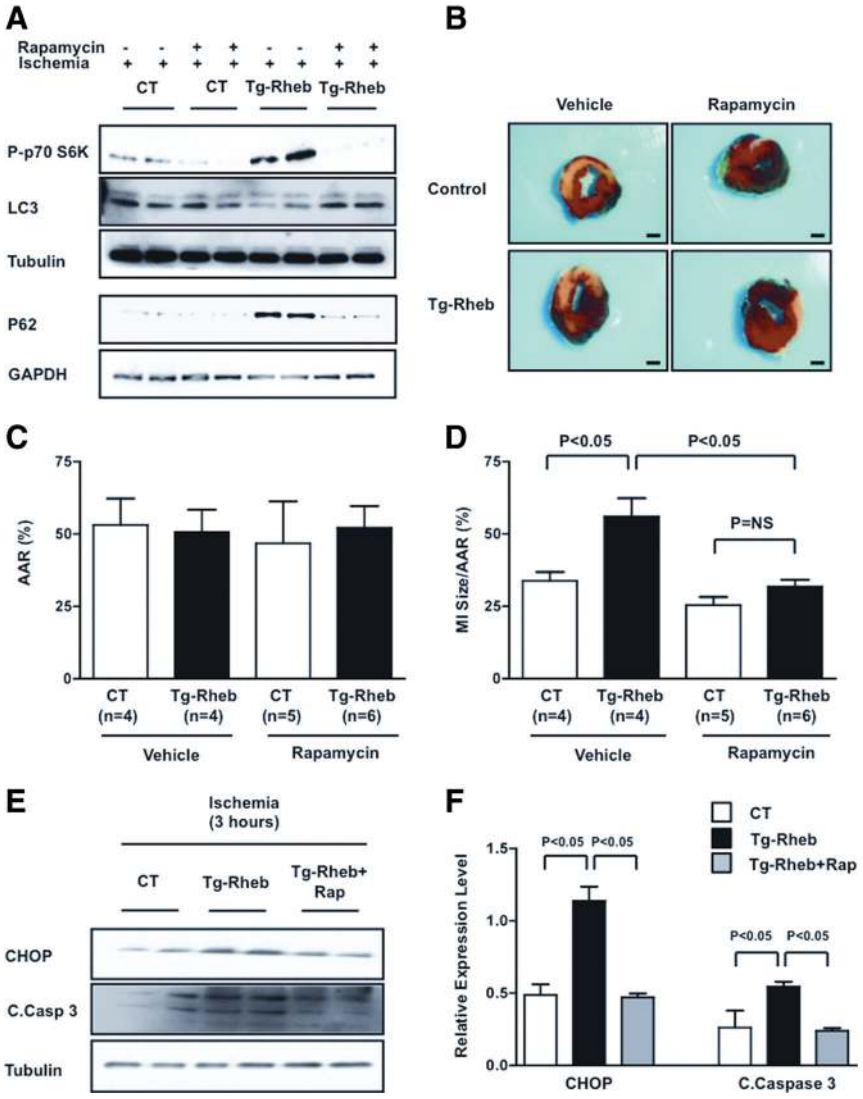

Figure 6. Rapamycin-induced autophagy limits myocardial damage in Rheb-overexpressing mice. **A**, Rapamycin (1 mg/kg) was administered intraperitoneally to Tg-Rheb and control mice (Rheb+/tTA−) 60 minutes before coronary ligation. $p70^{S6K}$ phosphorylation and LC3 expression levels were evaluated after 30 minutes of ischemia, whereas p62 expression levels were evaluated after 3 hours of ischemia. **B** through **D**, The MI/AAR ratio in Tg-Rheb and controls treated, or not treated, with rapamycin was evaluated. Bar=1 mm. **E** and **F**, CHOP expression and caspase-3 cleavage were also evaluated after 3 hours of ischemia. n=3 for each group. AAR indicates area at risk; MI, myocardial infarct; CT, control; CHOP, C/EBP homologous protein,

mice develop insulin resistance. HFD mice presented increases in mTOR-dependent IRS-1 phosphorylation (serine 636), which is a marker of decreased insulin sensitivity[18] at baseline (online-only Data Supplement Figure IXA). HFD mice showed a significant increase in left ventricular mass and left ventricular wall thickness but preserved left ventricular systolic function (online-only Data Supplement Table III). Both cell size and expression of atrial natriuretic factor, a fetal-type gene, were increased, suggesting that HFD mice develop cardiac hypertrophy (online-only Data Supplement Figure IXB through IXD). After prolonged (3 hours) ischemia, HFD mice exhibited a significantly greater MI size than CD mice (Figure 7A through 7C), which was accompanied by greater numbers of TUNEL-positive and Hairpin-2-positive cells (online-only Data Supplement Figure X), signifying that HFD increases myocardial susceptibility to ischemic injury. HFD mice also presented a greater percentage of hairpin-2–positive cells with respect to control mice after 30 minutes of ischemia (11.5±1.3% versus 4.2±1.0%, $P<0.05$).

In HFD mice, the activity of mTORC1 was greater at baseline and remained elevated during prolonged ischemia (Figure 7D and online-only Data Supplement Figure XIA). Thus, the suppression of mTORC1 in response to prolonged ischemia observed in CD mice was attenuated in HFD mice. Although the GTP-bound form of Rheb was significantly reduced during prolonged ischemia in CD mice, it was increased at baseline and not significantly diminished during prolonged ischemia in HFD mice (Figure 7E), suggesting that the activity of Rheb and mTORC1 is elevated at baseline and remains greater in HFD mice than in CD mice during prolonged ischemia. Intriguingly, the activity of AMPK, a negative regulator of the Rheb/mTORC1 pathway, was reduced in HFD mice both at baseline and during ischemia, as indicated by a reduction in its phosphorylation status. Conversely, it was activated in CD mice during ischemia (Figure 7D and online-only Data Supplement Figure XIA).

Consistent with activation of the mTORC1 pathway, autophagy in the heart was significantly suppressed in HFD mice both at baseline and during ischemia, as indicated by decreased LC3-II and increased p62 accumulation (Figure 7F, online-only Data Supplement Figure XIB and XIC). p62 mRNA expression was unchanged (0.84-fold versus CD

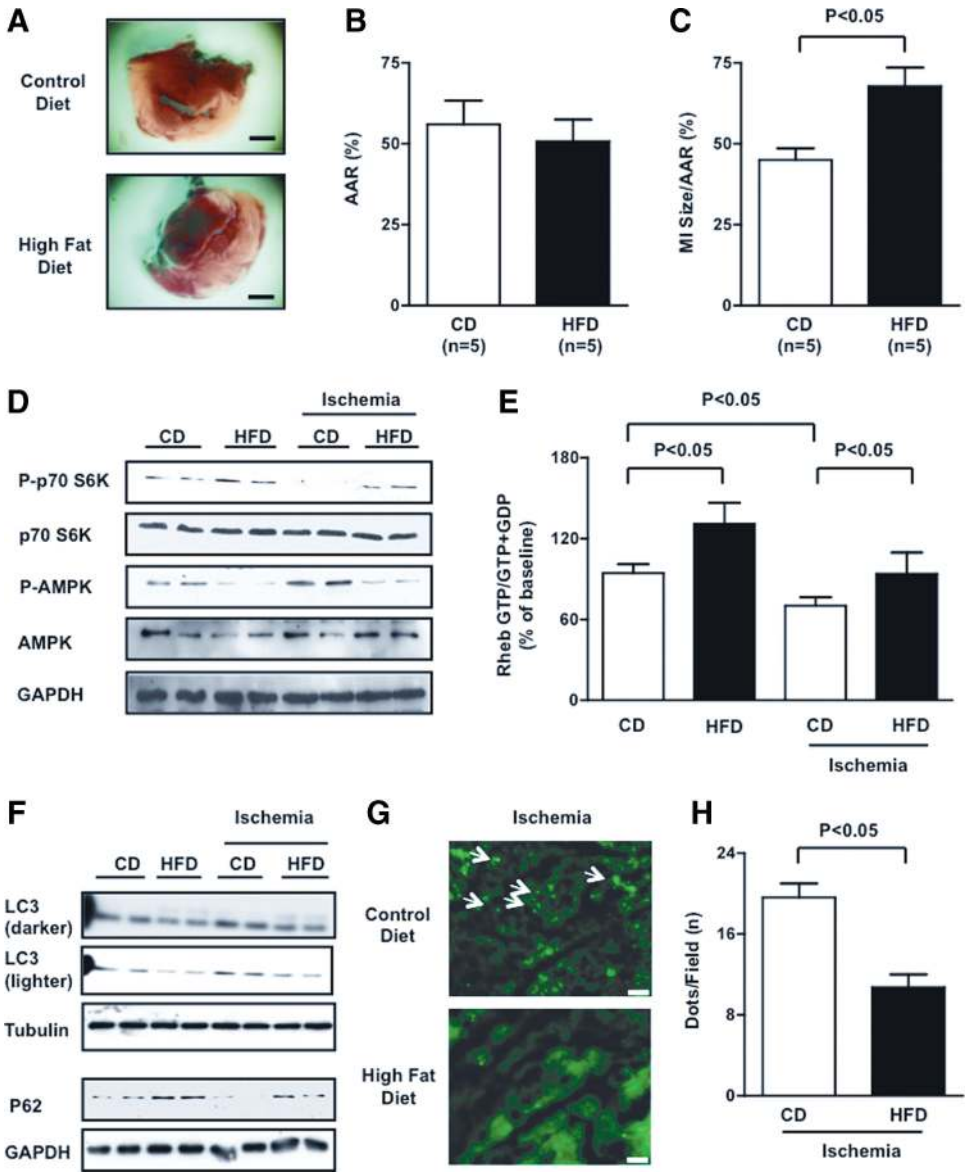

Figure 7. HFD-induced obesity is associated with greater myocardial injury and deregulated Rheb/mTORC1 activation. **A** through **C**, MI/AAR was evaluated in CD and HFD mice after ischemia. Bar=1 mm. **D**, Phosphorylation statuses of $p70^{S6K}$ and AMPK (Thr 172) were evaluated both at baseline and after 30 minutes of ischemia (densitometric analysis is shown in online-only Data Supplement Figure XIA). **E**, Myocardial Rheb-bound GTP content was evaluated in CD and HFD mice, both at baseline and after 30 minutes of ischemia. n=5 for each group. **F**, Myocardial autophagy in HFD mice was significantly inhibited in comparison with control mice, both at baseline and after 30 minutes (LC3-II levels) or 3 hours of ischemia (p62 levels). Representative immunoblots are presented, and densitometric analysis is reported in online-only Data Supplement Figure XIB and XIC. **G** and **H**, Tg-GFP-LC3 mice fed with CD or HFD were subjected to ischemia. Representative heart sections are shown. Bar=50 μm. Arrows indicate autophagosomes (**G**). The number of autophagosomes per microscopic field in the 2 groups after 30 minutes of ischemia is reported (**H**). n=4 each group. HFD indicates high-fat diet; CD, control diet; AAR, area at risk; MI, myocardial infarct.

mice, *P*=NS). Accumulation of autophagosomes, as evaluated by use of GFP-LC3 dots, was significantly less in HFD mice than in CD mice (Figure 7G and 7H). The number of GFP-LC3 dots was significantly reduced in HFD mice during ischemia, also after administration of chloroquine, which inhibits lysosomal enzyme activity. These data indicate reduced autophagosome formation in HFD mice (online-only Data Supplement Figure XID and XIE).

To investigate if deregulated activation of the mTORC1 pathway is responsible for the reduced tolerance to prolonged ischemia of HFD mice, we administered rapamycin to these animals and evaluated its effect on ischemic injury. As we observed with Tg-Rheb, rapamycin treatment increased autophagy (online-only Data Supplement Figure XIF) and significantly reduced the MI size of both HFD mice and CD mice (Figure 8A through 8C). Rapamycin administration failed to reduce ischemic injury in heterozygous *beclin-1* knockout mice (*beclin-1*+/−), in which autophagy cannot be activated, when fed with HFD (Figure 8D and 8E). These results indicate that autophagy reactivation mediates the beneficial effect of mTORC1 inhibition in HFD mice.

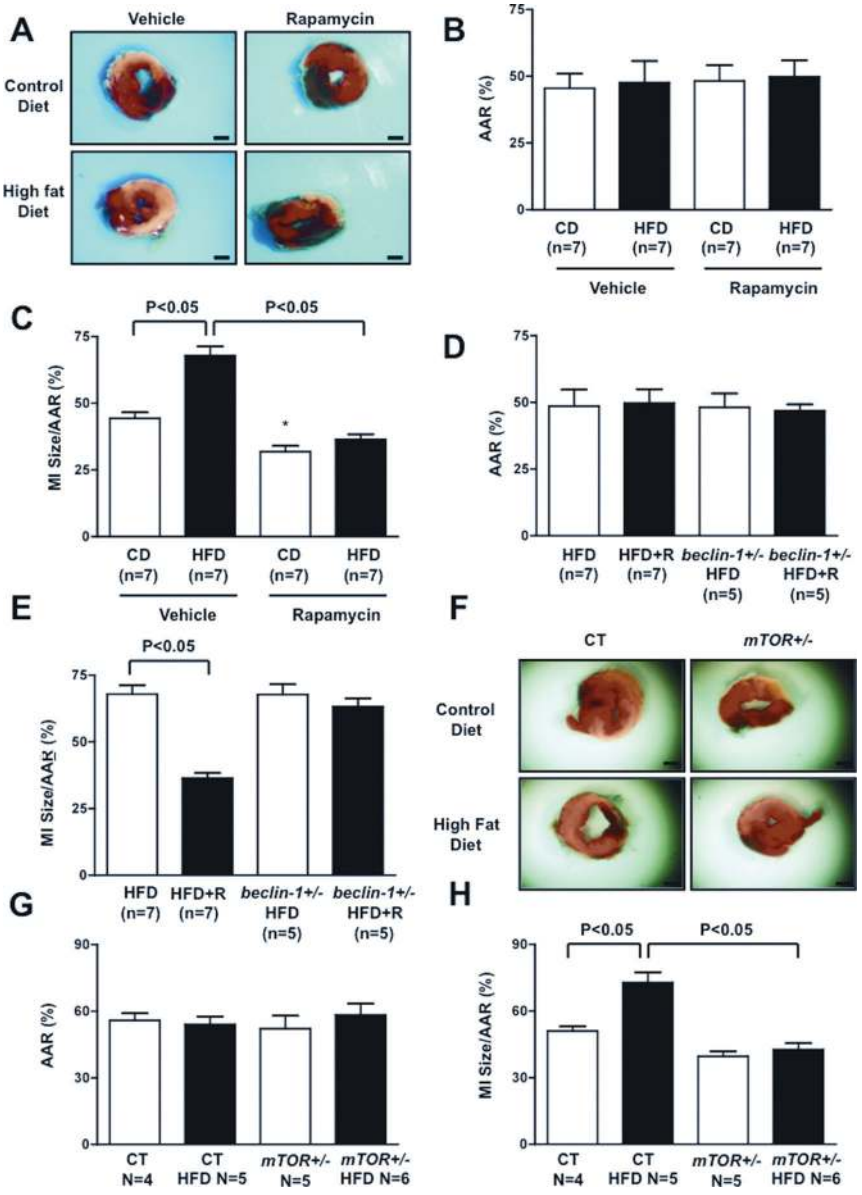

Figure 8. mTORC1 inhibition is protective in HFD mice through autophagy activation. **A** through **C**, Rapamycin (1 mg/kg) was administered intraperitoneally to HFD and CD mice 60 minutes before coronary ligation. Mice were subjected to 3 hours of ischemia. The MI/AAR ratio was evaluated. Bar=1 mm. *$P<0.05$ vs CD. **D** and **E**, Either control or *beclin-1*+/− mice fed with HFD were subjected to 3 hours of ischemia. The MI/AAR ratio was evaluated. *R* indicates rapamycin. **F** through **H**, After feeding with HFD or CD, tamoxifen (30 mg/kg) was administered to α-MHC-*MerCreMer-mTOR flox*/+ mice (*mTOR*+/−) and α-MHC-*MerCreMer-mTOR* +/+ mice (controls) for 7 days. The mice were subjected to 3 hours of ischemia. The MI/AAR ratio was evaluated. HFD indicates high-fat diet; CD, control diet; AAR, area at risk; MI, myocardial infarct; MHC, myosin heavy chain.

To further demonstrate that deregulated mTORC1 activation increases the ischemic susceptibility of HFD mice, we subjected mice, with inducible cardiac-specific heterozygous *mTOR* knockout, that were fed with HFD, to prolonged ischemia. This strategy allowed us to partially inhibit the mTOR pathway and to normalize the increased activation of mTORC1 observed in HFD mice. Tamoxifen was administered to α-myosin heavy chain promoter-*MerCreMer-mTOR flox*/+ mice (*mTOR*+/−) for 7 days. Cardiac mTOR protein levels were reduced in *mTOR*+/− mice 3 weeks after tamoxifen administration (online-only Data Supplement Figure XIIA). Cardiac *mTOR* deletion reduced mTORC1 activity and increased autophagy in *mTOR*+/− mice fed with control diet or HFD (online-only Data Supplement Figure XIIB through XIID). Remarkably, cardiac *mTOR* deletion reduced MI size in mice fed with control diet and HFD with respect to controls (Figure 8F through 8H). In summary, cardiac activation of the Rheb-mTORC1 pathway in HFD-induced obesity is detrimental during prolonged ischemia because of the inhibition of autophagy.

Discussion

We have demonstrated that Rheb is inhibited in response to GD and prolonged ischemia, and inhibition of Rheb, in turn, inhibits mTORC1 in CMs. Forced activation of Rheb in such conditions stimulates ATP depletion and ER stress by suppression of autophagy, thereby inducing cell death. Thus, Rheb acts as a sensor of energy stress and as a critical regulator of CM survival in response to energy starvation.

We have shown previously that both GD and ischemia in CMs and in the heart, respectively, induce suppression of mTOR.[19,20] It should be noted that mTOR is inhibited by both Rheb-dependent and -independent mechanisms.[19,20] For example, several upstream kinases, including AMPK and glycogen synthase kinase-3β, which indirectly regu-

late mTOR, inhibit Rheb through phosphorylation and consequent activation of GTPase-activating protein activity in TSC2.[2,3,8] It should be noted, however, that mTOR is also inhibited through Rheb-independent mechanisms, such as Akt-dependent phosphorylation of mTOR and PRAS40, and AMPK-dependent Raptor phosphorylation.[8] Our results indicate that Rheb interacts with mTOR, that Rheb is inhibited during GD and myocardial ischemia, and that its inactivation is required for mTORC1 inhibition. Conversely, neither overexpression of Rheb nor GD affected the activity of mTORC2. We therefore propose that Rheb acts as a central and direct regulator of mTORC1 during energy starvation in CMs.

Our results suggest that forced Rheb activation exacerbates cell death and apoptosis during GD and prolonged ischemia, but it does not affect cell survival at baseline. On the other hand, downregulation of Rheb increased survival of CMs during GD, intimating the involvement of endogenous Rheb in the regulation of survival/death during GD and prolonged ischemia. Previous studies have indicated that Rheb promotes cell survival and inhibits apoptotic cell death in response to stress in several cancer cells.[5,6] Activation of Rheb in unstressed conditions also induces hypertrophy without cell death in CMs (not shown). Thus, the function of Rheb in cells appears to be context dependent.

Importantly, we found that downregulation of mTORC1 mediates the protective effects of Rheb inhibition during energy deprivation, because depletion of Raptor but not of Rictor, which are the adaptor proteins of complex 1 and complex 2 of mTOR, respectively, increased survival of Rheb-overexpressing CMs during GD in vitro. In addition, pharmacological and genetic inhibition of mTORC1 reduced the susceptibility to ischemic myocardial damage of Rheb-overexpressing and obese mice, and a protective effect was also observed in control animals in vivo. These results suggest that Rheb is an obvious therapeutic surrogate of mTORC1, to achieve increased CM survival during energy deprivation.

The role of mTOR in regulating the stress response is poorly understood in terminally differentiated cell types such as CMs. In particular, the role of mTOR in the regulation of CM survival has been primarily investigated through indirect means, eg, the use of pharmacological inhibitors, which may have mTOR-independent effects.[19,20] In addition, the role of mTOR in cardiac stress has been mostly studied in animal models of chronic ventricular remodeling in which mTORC1 is activated, whereas we observed mTORC1 inhibition during CM energy deprivation.[9–11] Interestingly, mTORC1 activation has been indicated as protective during cardiac mechanical overload.[9,11] On the other hand, in our study, we demonstrated that selective and direct mTORC1 activation is detrimental during acute cardiac energy deprivation, whereas both pharmacological and genetic mTORC1 inhibitions are protective. In particular, we provided the first evidence that genetic mTOR inhibition is protective during myocardial ischemia. Thus, the function of mTORC1 in CMs appears to be context dependent. mTORC1 activation might be required for cell growth in response to mechanical overload, whereas mTORC1 inhibition is important for preservation of energy status in response to energy deprivation.

Rheb inhibition during energy deprivation is required for autophagy activation, which is protective in this condition. In fact, suppression of autophagy by knockdown of Beclin-1 completely abrogated the protective effect of Rheb knockdown in CMs during GD. Restoration of autophagy through treatment with trehalose or overexpression of Atg7, which stimulates autophagy through mTOR-independent mechanisms, significantly reduced CM death induced by forced Rheb activation. Therefore, although it is still debated whether autophagy is protective or detrimental during cardiac stress,[24] we have demonstrated that Rheb-regulated autophagy is protective during CM nutrient starvation and ischemia. In particular, we showed that Rheb-regulated autophagy is protective through the preservation of ATP content and reduction of misfolded protein accumulation, namely ER stress.

Rheb-induced inhibition of autophagy was accompanied by downregulation of Atg7 protein levels. Overexpression of Atg7 was sufficient to restore autophagy and to suppress Rheb-induced cell death during GD, suggesting that Rheb regulates autophagy, in part, through Atg7. mTORC1 was suggested to modulate autophagy through Ulk1/2 regulation.[21] The role of Ulk1/2 in mediating expression of Atg7 remains to be elucidated.

Interestingly, inadvertent activation of the Rheb/mTORC1 pathway is observed in HFD-induced obesity. Obesity is characterized by glucose intolerance and dyslipidemia, and it is associated with an increased susceptibility to myocardial ischemia.[13–16] We demonstrated that autophagy is reduced in the hearts of mice with HFD-induced obesity. These mice exhibited exacerbated myocardial injury in response to prolonged ischemia, which was normalized by rapamycin treatment or genetic mTOR inhibition, suggesting that increased mTORC1 activity may be responsible for the increased susceptibility. Remarkably, inhibition of Beclin-1 was associated with the failure of pharmacological mTORC1 inhibition to reduce ischemic injury in HFD mice, indicating that reactivation of autophagy is the crucial mechanism mediating the beneficial effects of mTORC1 inhibition in HFD-induced obesity.

Severe obesity and metabolic syndrome are associated with increased cardiovascular risk events and a poor prognosis in patients after acute MI.[12,14,15,25,26] If our results hold true in humans, it may be helpful to treat patients with obesity and metabolic syndrome by use of pharmacological inhibitors of Rheb or mTORC1 to stimulate autophagy during an acute episode of myocardial ischemia. Our results are also supported by an interesting previous study that showed that obesity increases vascular senescence and vascular dysfunction in response to mTOR activation.[27]

Other previous studies showed increased basal mTORC1 activity in the liver,[17,28] adipose tissue,[29] vasculature,[27] skeletal muscle,[17,28,30,31] and cardiac muscle[32–34] in both genetic and diet-induced models of obesity and dysmetabolic conditions. AMPK inhibition has been proposed as the main intracellular mechanism leading to mTORC1 activa-

tion.[18,30–34] Our study extends this previous evidence, suggesting that Rheb is involved in the activation of mTORC1 induced by AMPK downregulation.

Several stimuli may enhance the activity of the Rheb/mTORC1 pathway in the tissues of obese and dysmetabolic animals. High caloric intake may represent one possible cause. High levels of circulating and cardiac lipids may also represent potential mechanisms. In addition, increases in circulating insulin, amino acids, cytokines, and adipokines may contribute to the increased Rheb/mTORC1 activity in HFD mice.[17,18,28,31,32,35]

In summary, our study demonstrates that inactivation of Rheb protects CMs during energy deprivation through activation of autophagy, reduction of energy expenditure, and attenuation of ER stress (online-only Data Supplement Figure XIIE). Rheb and mTORC1 may represent therapeutic targets to reduce myocardial damage during acute myocardial ischemia, particularly in patients with obesity and metabolic syndrome.

Acknowledgments

The authors thank Christopher D. Brady and Daniela Zablocki for their critical revisions of the article.

Sources of Funding

Dr Sciarretta is supported by the American Heart Association Founders Affiliate FDA Spring 2010 postdoctoral fellowship 10POST4260019. This work was supported in part by US Public Health Service grants HL59139, HL67724, HL69020, HL91469, HL102738, and AG27211 and by the Foundation of Leducq Transatlantic Network of Excellence.

Disclosures

None.

References

1. Velagaleti RS, Pencina MJ, Murabito JM, Wang TJ, Parikh NI, D'Agostino RB, Levy D, Kannel WB, Vasan RS. Long-term trends in the incidence of heart failure after myocardial infarction. *Circulation*. 2008; 118:2057–2062.
2. Inoki K, Ouyang H, Zhu T, Lindvall C, Wang Y, Zhang X, Yang Q, Bennett C, Harada Y, Stankunas K, Wang CY, He X, MacDougald OA, You M, Williams BO, Guan KL. TSC2 integrates Wnt and energy signals via a coordinated phosphorylation by AMPK and GSK3 to regulate cell growth. *Cell*. 2006;126:955–968.
3. Aspuria PJ, Sato T, Tamanoi F. The TSC/Rheb/TOR signaling pathway in fission yeast and mammalian cells: temperature sensitive and constitutive active mutants of TOR. *Cell Cycle*. 2007;6:1692–1695.
4. Karassek S, Berghaus C, Schwarten M, Goemans CG, Ohse N, Kock G, Jockers K, Neumann S, Gottfried S, Herrmann C, Heumann R, Stoll R. Ras homolog enriched in brain (Rheb) enhances apoptotic signaling. *J Biol Chem*. 2010;285:33979–33991.
5. Babcock JT, Quilliam LA. Rheb/mTOR Activation and regulation in cancer: novel treatment strategies beyond rapamycin. *Curr Drug Targets*. 2011;12:1223–1231.
6. Ma D, Bai X, Zou H, Lai Y, Jiang Y. Rheb GTPase controls apoptosis by regulating interaction of FKBP38 with Bcl-2 and Bcl-XL. *J Biol Chem*. 2010;285:8621–8627.
7. Inoki K, Li Y, Xu T, Guan KL. Rheb GTPase is a direct target of TSC2 GAP activity and regulates mTOR signaling. *Genes Dev*. 2003;17: 1829–1834.
8. Sengupta S, Peterson TR, Sabatini DM. Regulation of the mTOR complex 1 pathway by nutrients, growth factors, and stress. *Mol Cell*. 2010;40:310–322.
9. Zhang D, Contu R, Latronico MV, Zhang JL, Rizzi R, Catalucci D, Miyamoto S, Huang K, Ceci M, Gu Y, Dalton ND, Peterson KL, Guan KL, Brown JH, Chen J, Sonenberg N, Condorelli G. MTORC1 regulates cardiac function and myocyte survival through 4E-BP1 inhibition in mice. *J Clin Invest*. 2010;120:2805–2816.
10. Buss SJ, Muenz S, Riffel JH, Malekar P, Hagenmueller M, Weiss CS, Bea F, Bekeredjian R, Schinke-Braun M, Izumo S, Katus HA, Hardt SE. Beneficial effects of Mammalian target of rapamycin inhibition on left ventricular remodeling after myocardial infarction. *J Am Coll Cardiol*. 2009;54:2435–2446.
11. Song X, Kusakari Y, Xiao CY, Kinsella SD, Rosenberg MA, Scherrer-Crosbie M, Hara K, Rosenzweig A, Matsui T. mTOR attenuates the inflammatory response in cardiomyocytes and prevents cardiac dysfunction in pathological hypertrophy. *Am J Physiol Cell Physiol*. 2010; 299:C1256–C1266.
12. Flegal KM, Carroll MD, Ogden CL, Curtin LR. Prevalence and trends in obesity among US adults, 1999–2008. *JAMA*. 2010;303:235–241.
13. Clavijo LC, Pinto TL, Kuchulakanti PK, Torguson R, Chu WW, Satler LF, Kent KM, Suddath WO, Pichard AD, Waksman R. Metabolic syndrome in patients with acute myocardial infarction is associated with increased infarct size and in-hospital complications. *Cardiovasc Revasc Med*. 2006;7:7–11.
14. Zeller M, Steg PG, Ravisy J, Laurent Y, Janin-Manificat L, L'Huillier I, Beer JC, Oudot A, Rioufol G, Makki H, Farnier M, Rochette L, Verges B, Cottin Y. Prevalence and impact of metabolic syndrome on hospital outcomes in acute myocardial infarction. *Arch Intern Med*. 2005;165: 1192–1198.
15. Abdulla J, Kober L, Abildstrom SZ, Christensen E, James WP, Torp-Pedersen C. Impact of obesity as a mortality predictor in high-risk patients with myocardial infarction or chronic heart failure: a pooled analysis of five registries. *Eur Heart J*. 2008;29:594–601.
16. du Toit EF, Smith W, Muller C, Strijdom H, Stouthammer B, Woodiwiss AJ, Norton GR, Lochner A. Myocardial susceptibility to ischemic-reperfusion injury in a prediabetic model of dietary-induced obesity. *Am J Physiol Heart Circ Physiol*. 2008;294:H2336–H2343.
17. Khamzina L, Veilleux A, Bergeron S, Marette A. Increased activation of the mammalian target of rapamycin pathway in liver and skeletal muscle of obese rats: possible involvement in obesity-linked insulin resistance. *Endocrinology*. 2005;146:1473–1481.
18. Um SH, D'Alessio D, Thomas G. Nutrient overload, insulin resistance, and ribosomal protein S6 kinase 1, S6K1. *Cell Metab*. 2006;3:393–402.
19. Matsui Y, Takagi H, Qu X, Abdellatif M, Sakoda H, Asano T, Levine B, Sadoshima J. Distinct roles of autophagy in the heart during ischemia and reperfusion: roles of AMP-activated protein kinase and Beclin 1 in mediating autophagy. *Circ Res*. 2007;100:914–922.
20. Zhai P, Sciarretta S, Galeotti J, Volpe M, Sadoshima J. Differential roles of GSK-3β during myocardial ischemia and ischemia/reperfusion. *Circ Res*. 2011;109:502–511.
21. Ravikumar B, Futter M, Jahreiss L, Korolchuk VI, Lichtenberg M, Luo S, Massey DC, Menzies FM, Narayanan U, Renna M, Jimenez-Sanchez M, Sarkar S, Underwood B, Winslow A, Rubinsztein DC. Mammalian macroautophagy at a glance. *J Cell Sci*. 2009;122:1707–1711.
22. Yang L, Li P, Fu S, Calay ES, Hotamisligil GS. Defective hepatic autophagy in obesity promotes ER stress and causes insulin resistance. *Cell Metab*. 2010;11:467–478.
23. Sarkar S, Davies JE, Huang Z, Tunnacliffe A, Rubinsztein DC. Trehalose, a novel mTOR-independent autophagy enhancer, accelerates the clearance of mutant huntingtin and alpha-synuclein. *J Biol Chem*. 2007; 282:5641–5652.
24. Hamacher-Brady A, Brady NR, Gottlieb RA. Enhancing macroautophagy protects against ischemia/reperfusion injury in cardiac myocytes. *J Biol Chem*. 2006;281:29776–29787.
25. Romero-Corral A, Montori VM, Somers VK, Korinek J, Thomas RJ, Allison TG, Mookadam F, Lopez-Jimenez F. Association of bodyweight with total mortality and with cardiovascular events in coronary artery disease: a systematic review of cohort studies. *Lancet*. 2006;368: 666–678.
26. Aronson D, Nassar M, Goldberg T, Kapeliovich M, Hammerman H, Azzam ZS. The impact of body mass index on clinical outcomes after acute myocardial infarction. *Int J Cardiol*. 2010;145:476–480.
27. Wang CY, Kim HH, Hiroi Y, Sawada N, Salomone S, Benjamin LE, Walsh K, Moskowitz MA, Liao JK. Obesity increases vascular senescence and susceptibility to ischemic injury through chronic activation of Akt and mTOR. *Sci Signal*. 2009;2:ra11.
28. Um SH, Frigerio F, Watanabe M, Picard F, Joaquin M, Sticker M, Fumagalli S, Allegrini PR, Kozma SC, Auwerx J, Thomas G. Absence of

S6K1 protects against age- and diet-induced obesity while enhancing insulin sensitivity. *Nature*. 2004;431:200–205.
29. Ranieri SC, Fusco S, Panieri E, Labate V, Mele M, Tesori V, Ferrara AM, Maulucci G, De Spirito M, Martorana GE, Galeotti T, Pani G. Mammalian life-span determinant p66shcA mediates obesity-induced insulin resistance. *Proc Natl Acad Sci U S A*. 2010;107:13420–13425.
30. Drake JC, Alway SE, Hollander JM, Williamson DL. AICAR treatment for 14 days normalizes obesity-induced dysregulation of TORC1 signaling and translational capacity in fasted skeletal muscle. *Am J Physiol Regul Integr Comp Physiol*. 2010;299:R1546–R1554.
31. Rivas DA, Yaspelkis BB, III, Hawley JA, Lessard SJ. Lipid-induced mTOR activation in rat skeletal muscle reversed by exercise and 5′-aminoimidazole-4-carboxamide-1-beta-D-ribofuranoside. *J Endocrinol*. 2009;202:441–451.
32. Glazer HP, Osipov RM, Clements RT, Sellke FW, Bianchi C. Hypercholesterolemia is associated with hyperactive cardiac mTORC1 and mTORC2 signaling. *Cell Cycle*. 2009;8:1738–1746.
33. Sung MM, Koonen DP, Soltys CL, Jacobs RL, Febbraio M, Dyck JR. Increased CD36 expression in middle-aged mice contributes to obesity-related cardiac hypertrophy in the absence of cardiac dysfunction. *J Mol Med (Berl)*. 2011;89:459–469.
34. Turdi S, Kandadi MR, Zhao J, Huff AF, Du M, Ren J. Deficiency in AMP-activated protein kinase exaggerates high fat diet-induced cardiac hypertrophy and contractile dysfunction. *J Mol Cell Cardiol*. 2011;50:712–722.
35. Hay N, Sonenberg N. Upstream and downstream of mTOR. *Genes Dev*. 2004;18:1926–1945.

CLINICAL PERSPECTIVE

The incidence of heart failure after acute myocardial infarction (MI) remains very high in patients. This highlights the necessity to clarify the mechanism regulating the survival and death of cardiomyocytes in response to ischemia and to find new cardioprotective therapies reducing ischemic injury. We discovered that Rheb, a small GTP-binding protein, plays a pivotal role in regulating the survival of cardiomyocytes during prolonged myocardial ischemia. Rheb activity is reduced in the ischemic heart, thereby causing the suppression of the mTORC1 pathway. Inhibition of the Rheb/mTORC1 pathway is an adaptive response during ischemia, because forced restoration of cardiac Rheb activity is detrimental under this condition. Rheb inhibition is required for the activation of autophagy, an intracellular degradation process for proteins and organelles, which is protective during energy stress through preservation of cellular energy and relief of ER stress. We discovered that obesity and metabolic syndrome (Ob/MS) are associated with cardiac activation of Rheb/mTORC1 at baseline and during ischemia. In obese mice, autophagy in the heart was suppressed and ischemic injury was exacerbated. Remarkably, inhibition of mTORC1 restores autophagy and reduces infarct size in these animals after prolonged ischemia. Thus, our results suggest that Rheb and mTORC1 may be promising therapeutic targets to reduce myocardial damage after prolonged ischemia in patients with Ob/MS who display deregulated activation of the Rheb/TORC1 pathway and consequent inhibition of autophagy.

SUPPLEMENTAL MATERIAL

Supplemental Methods

Primary cultures of neonatal rat ventricular cardiomyocytes and reagents

Primary cultures of ventricular cardiomyocytes were prepared from 1-day-old Crl: (WI) BR Wistar rats (Charles River Laboratories). A cardiomyocyte-rich fraction was obtained by centrifugation through a discontinuous Percoll gradient. Cells were cultured in a complete medium (cardiomyocyte) containing Dulbecco's modified Eagle's medium (DMEM)/F-12 supplemented with 5% horse serum, 4 μg/ml transferrin, 0.7 ng/ml sodium selenite (Life Technologies, Inc.), 2 g/liter bovine serum albumin (fraction V), 3 mM pyruvic acid, 15 mM HEPES, 100 μM ascorbic acid, 100 μg/ml ampicillin, 5 μg/ml linoleic acid and 100 μM 5-bromo-2'-deoxyuridine (Sigma). Trehalose and rapamycin were purchased from Sigma.

Generation of Tg-Rheb mice

A tetracycline-responsive binary α-MHC transgene system was used to allow temporally regulated expression of wild-type Rheb in cardiomyocytes [1]. Mice were generated on a FVB background. Doxycycline was administered in the food with a special diet formulated by Purina (625 mg/kg in pellets). In the experiments that required Rheb protein induction, doxycycline was removed from the food at 3-4 weeks of life, resulting in induced expression of Rheb a few weeks later. All experimental procedures with animals were approved by the Institutional Animal Care and Use Committee of the University of Medicine and Dentistry of New Jersey.

Construction of adenoviruses

Recombinant adenovirus vectors were constructed as described [2]. pBHGloxΔE1,3Cre (Microbix), including the ΔE1 adenoviral genome, was co-transfected with the pDC shuttle vector containing the gene of interest into 293 cells. We made replication-defective human adenovirus type 5 (devoid of E1) harboring full length wild-type Rheb cDNA (Ad-Rheb) and full length wild-type Atg7 (Ad-Atg7), and

we used adenovirus harboring beta-galactosidase (Ad-LacZ) as a control. For the construction of short hairpin RNA (sh-RNA) adenoviral expression vectors, p*Silencer* 1.0-U6 expression vector was purchased from Ambion. The U6 RNA polymerase III promoter and the polylinker region were subcloned into the adenoviral shuttle vector pDC311 (Microbix). The hairpin-forming oligos of Rheb, Beclin-1, Raptor, Rictor and TSC2 rat cDNA and their antisenses with ApaI and Hind III overhangs were synthesized, annealed and subcloned distal to the U6 promoter. Recombinant adenoviruses were generated using homologous recombination in 293 cells. Cardiomyocytes were transduced with adenovirus for 48 hours in case of overexpression, and for 96 hours for sh-RNA-mediated knock-down.

Echocardiography

Echocardiography was performed after mice were anesthetized with 12 µl/g body weight of 2.5% Avertin, as described previously [2].

Prolonged ischemia

Pathogen-free mice were housed in a temperature-controlled environment with 12 hr light/dark cycles, where they received food and water ad libitum. Mice were anesthetized by intraperitoneal injection of pentobarbital sodium (60 mg/kg). A rodent ventilator (model 683;
Harvard Apparatus Inc) was used with 65% oxygen during the surgical procedure. The animals were kept warm using heat lamps and heating pads. Rectal temperature was monitored and maintained between 36.5 and 37.5°C. The chest was opened by a horizontal incision through the muscle between the ribs (third intercostal space). Ischemia was achieved by ligating the anterior descending branch of the left coronary artery (LAD) using an 8-0 nylon suture, with a silicon tubing (1 mm OD) placed on top of the LAD, 2 mm below the border between left atrium and left ventricle (LV). Regional ischemia was confirmed by ECG change (ST elevation).

Assessment of area at risk and infarct size

After 3 hours of ischemia, the animals were reanesthetized and intubated, and the chest was opened. After arresting the heart at the diastolic phase by KCl injection, the ascending aorta was cannulated and perfused with saline to wash out blood. To demarcate the ischemic area at risk (AAR), Alcian blue dye (1%) was perfused into the aorta and coronary arteries. Hearts were excised, and LVs were sliced into 1-mm thick cross sections. The heart sections were then incubated with a 1% triphenyltetrazolium chloride (TTC) solution at 37°C for 10 min. The infarct area (pale), the AAR (not blue), and the total LV area from both sides of each section were measured using ImageJ (NIH) and Adobe Photoshop (Adobe Systems Inc.), and the values obtained were averaged. The percentages of area of infarction and AAR of each section were multiplied by the weight of the section and then totaled from all sections. AAR/LV and infarct area/AAR were expressed as percentages. The extent of necrosis after 30 minutes of ischemia was quantified through Hairpin-2 staining (See below), since TTC staining is less accurate for the assessment of infarct size after this period of time[3].

High fat diet (HFD) mice feeding

C57BL/6J wild-type mice, heterozygous *Beclin-1* systemic knock-out mice, conditional *mTOR* knock-out mice crossed with α-MHC-*MerCreMer* mice (C57BL/J background), and heterozygous GFP-LC3 transgenic mice (C57BL/6J background, strain GFP-LC3#53, RIKEN BioResource Center) containing a rat LC3-GFP fusion under control of the chicken ß-actin promoter, were fed ad libitum with HFD (Research Diets D12492) for 18-20 weeks. A control group of mice matched for age and gender was fed with control diet for the same period of time.

Mice hematochemical analysis

Serum levels of glucose, cholesterol, triglycerides and non-esterified fatty acids (NEFA) in mice fed with control diet and high-fat diet were assessed by *in vitro* enzymatic colorimetric methods (Wako), according to the manufacturer's instructions. Serum levels of insulin were assessed with an ELISA assay (Crystalchem).

Evaluation of apoptosis in tissue sections

DNA fragmentation was detected *in situ* using the TUNEL assay, as described previously [2]. Briefly, deparaffinized sections were incubated with proteinase K, and DNA fragments were labeled with fluorescein-conjugated dUTP using TdT (Roche Molecular Biochemicals). Nuclear density was determined by manual counting of DAPI-stained nuclei in six fields for each animal using the 40x objective, and the number of TUNEL-positive nuclei was counted by examining the entire section using the same power objective.

TUNEL staining in cultured cardiomyocytes

Myocytes were fixed in PBS containing 4% paraformaldehyde. Staining was performed using the In Situ Cell Death Detection kit (Roche).

Assessment of necrosis *in vivo* with Hairpin-2 staining

A double-stranded DNA fragment with blunt ends was prepared as previously described [4, 5]. Polymerase chain reaction (PCR) with Pfu Ultra polymerase was performed with 16.6 μM Texas Red-12-dUTP (Molecular Probes), 16.6 μM dTTP, 50 μM dATP, 50 μM dCTP and 50 μM dGTP. The Pfu probe recognizes a form of DNA damage characterized by cleavage of multiple DNA fragments with blunt ends, typically observed in necrotic cell death [6]. Heart sections were deparaffinized with xylene, rehydrated in graded alcohol concentrations, briefly washed in water and then treated with proteinase K (50 μg/ml) in PBS for 45 minutes at 37°C. After washing with PBS, a mix of 50 mM Tris-HCl, pH 7.8, 10 mM MgCl2, 10 mM, DTT, 1 mM ATP, 25 μg/ml BSA, 15% polyethylene glycol (8,000 mol wt, Sigma), 1 μg/ml Texas red-labeled DNA fragment and 250 U/ml DNA T4 ligase (Roche) was added. Sections were then placed in a humidified box for 16 hours. The sections were thoroughly washed in 70°C water and observed under a fluorescent microscope immediately after counterstaining with 10 μg/ml 4,6-diamidino-2-phenylindole (DAPI).

Cell size evaluation and histological analysis

Heart specimens were fixed with 10 % neutral buffered formalin, embedded in paraffin, and sectioned at 6-μm thickness. Cell size was assessed through wheat germ agglutinin staining, as previously described [2]. Immunofluorescent staining was performed with reagents and protocols previously described [7]. Cardiac myocytes were stained with anti-troponin T antibody. Alexa 488- and Alexa 594-conjugated secondary antibodies (Invitrogen) were used. Nuclei were stained with DAPI.

Viability of the cells

Viability of the cells was measured by Cell Titer Blue (CTB) assays (Promega). In sum, cardiomyocytes ($1x10^5$ per 100 μl) were seeded onto 96-well dishes. After 24 hours, the medium was changed to a serum free medium. Cardiomyocytes were transduced with adenovirus harboring Rheb, Atg7 or LacZ for 36-48 hours, or shRNA against Rheb, TSC2, Beclin-1 or scramble shRNA for 96 hours, and then changed to a glucose free medium for the time required by the experiment. Viable cell numbers were measured by the CTB assay. The CTB assays were performed according to the supplier's protocol. In vitro, necrosis was assessed through propidium iodide staining as previously described [4]

Evaluation of autophagy

Autophagy was assessed by three different methods: LC3-II accumulation, p62 accumulation and autophagosome formation [8, 9]. *In vivo*, LC3-II accumulation was evaluated in the early phase of ischemia (30 minutes), since LC3-II may be degraded and may not be reliable in the later phase [9]. Autophagy in the later phase of ischemia was assessed by accumulation of p62, a protein known to be degraded by autophagy [9], since p62 accumulation represents a more stable marker of autophagy. Autophagosome formation *in vivo* was evaluated by counting GFP-LC3 dots in at least seven independent fields of heart sections from Tg-GFP-LC3 mice. These mice selectively express LC3

conjugated to a green fluorescent protein in the heart [8]. GFP-LC3 dots were also evaluated after chloroquine administration (10 mg/kg i.p.) to evaluate autophagic flux, as previously described [10]. For analysis of autophagosome formation *in vitro*, cardiomyocytes were grown on gelatinized coverslips. Myocytes were transduced with Ad-GFP-LC3, viruses that express GFP-LC3, for 48 hours. Samples were mounted using a SlowFade Light Antifade Kit (MolecularProbes), and the fluorescence of GFP-LC3 was observed under a fluorescence microscope. The number of cells with GFP-LC3 dots was counted in at least seven independent visual fields.

Gene expression analysis

mRNA expression of p62, atrial natriuretic factor (ANF) and GAPH (loading control) was evaluated with quantitative real time PCR, as described[4]. The following primers were used: p62 sense 5'-CAGGCGCACTACCGCGATGA-3', antisense 5'-TCGCACACGCTGCACAGGTC-3'; ANF sense 5'-ATGGGCTCCTTCTCCATCAC-3', antisense 5'-ATCTTCGGTACCGGAAGCTG-3'; and GAPDH sense 5'-TTCTTGTGCAGTGCCAGCCTCGTC-3', antisense 5'-TAGGAACACGGAAGGCCATGCCAG-3';

Immunoblot analysis, antibodies and reagents

For immunoblot analyses, heart homogenates and cardiomyocyte lysates were prepared in a RIPA lysis buffer containing 50 mM Tris·HCl (pH 7.5), 150 mM NaCl, 1% Triton X-100, 0.1% SDS, 0.5% deoxycholic acid, 1 mM EDTA, 0.1 mM Na_3VO_4, 1 mM NaF, 50 μM phenylmethylsulfonyl fluoride (PMSF), 5 μg/ml aprotinin and 5 μg/ml leupeptin. The antibodies used include anti-Rheb (Cell Signaling Technology and Santa Cruz), phospho-p70S6K (Thr389, Cell Signaling Technology), p70S6K (Santa Cruz), phospho-4E-BP1 (Thr37/46, Cell Signaling Technology), 4E-BP1 and mTOR (Cell Signaling Technology), TSC2 (Santa Cruz), p62 (American Research Products, Inc.), LC3 (MBL), Bip (Cell Signaling Technology), phospho-PERK (Thr980, Cell Signaling Technology), CHOP (Santa Cruz), Caspase-12 and cleaved Caspase-3 (Cell

Signaling Technology), Beclin-1 (Pharmingen), Atg4 (MBL), Atg5 (MBL), Atg7 (MBL), Ulk1 (Abcam), phospho-IR (Tyr11262/3, Santacruz), phospho-IRS1 (Tyr989, Ser636, Santacruz), IR and IRS-1 (Cell Signaling Technology), phospho-Akt1 (Ser473, Millipore), Akt1 (Cell Signaling Technology), GAPDH (Sigma) and tubulin (Sigma).

Measurement of Rheb activity

Endogenous Rheb activity is commonly evaluated by the ratio of GTP and GDP bound to Rheb, as Rheb is highly active when it is rich in GTP [11]. Rheb-bound GTP and GDP amounts were assessed according to a previously described luminometric method [12, 13]. This method represents a well-established assay for the measurement of the activity of GTP-binding proteins [14, 15].

Proteins were extracted from cultured cardiomyocytes or mouse heart specimens in an ice-cold HEPES-based buffer containing 10 mM $MgCl_2$, protease inhibitors and 1% Igepal CA-630 [15]. The anti-Rheb C antibody or control IgG was added to the samples, which were shaken at 4°C overnight in the presence of 500 mM NaCl, 0.5% deoxycholate and 0.05% SDS. Protein G-agarose was then added to each sample. After shaking for 2 hours at 4°C, the agarose beads were washed four times in lysis buffer containing NaCl and detergents, and two times in 20 mM TrisPO_4, 5 mM Mg2SO_4. The beads were resuspended in 20 mM TrisPO_4, 1mM DTT, 1 mM EDTA, and heated at 100°C for 3 min to elute GTP and GDP bound to the immunoprecipitated Rheb. In each sample, GTP and the sum of GTP plus GDP were measured in coupled enzymatic assays [15]. GTP was converted to ATP by nucleoside diphosphate kinase (3 mu) in the presence of ADP (10 pmol), and the resulting ATP was measured by the luciferase method (4 mmol of luciferin and $8x10^8$ light units of luciferase). The sum of GTP plus GDP was measured by converting GDP to GTP using pyruvate kinase (3 mu) and phosphoenolpyruvate (50 μM). GTP, which at this point represents the sum of GDP plus GTP, was measured as described above. The GTP/GTP+GDP ratio was then calculated by the ratio of the emitted light in the two reactions.

Measurement of intracellular ATP content

Intracellular ATP content was measured using an ATP Bioluminescent Assay Kit (Sigma). Cells were scraped with PBS, and then half of them were used for protein content assay and the other half for ATP content measurement. For the latter assay, cells were lysed in the somatic-cell ATP-releasing agent, and the lysates were assayed according to the manufacturer's instructions, using a 1:625 dilution of the ATP assay mix. Light emitted was measured using a luminometer and was then normalized for protein content of the sample. For ATP content assays in myocardial tissue, heart specimens of equal weights were directly lysed in the somatic-cell ATP-releasing agent, and the lysates were assayed as described above.

Supplemental Tables

Table I. Echocardiographic parameters of Tg-Rheb.

	Parameters	NTg (N=4)	Tg-Rheb (N=4)
Echocardiographic parameters	SWTd (mm)	0.91 ± 0.05	0.94 ± 0.03
	LVEDD (mm)	3.89 ± 0.10	3.92 ± 0.11
	PWTd (mm)	0.87 ± 0.05	0.89 ± 0.03
	SWTs (mm)	1.48 ± 0.11	1.51 ± 0.09
	LVESD (mm)	2.31 ± 0.11	2.29 ± 0.05
	PWTs (mm)	1.21 ± 0.05	1.30 ± 0.08
	FS (%)	40.49 ± 1.23	41.38 ± 1.05

SWTd: diastolic septum wall thickness; LVEDD: left ventricular end-diastolic diameter; PWTd: diastolic posterior wall thickness. Data is presented as (mean ± SEM).

Table II. Body weight and hematochemical tests in HFD mice as compared with CD mice.

Parameters	Control diet (N=15)	High fat diet (N=15)
Body weight (g)	26.8 ± 1.0	54.6 ± 3.3*
Glucose (mg/dl)	112.9 ± 6.2	176.0 ± 17.3*
Insulin (ng/ml)	0.23 ± 0.01	0.43 ± 0.02*
HOMA Index	1.8 ± 0.22	5.8 ± 0.65*
Total cholesterol (mg/dl)	84.1 ± 3.1	126.1 ± 8.0*
Trygliceride (mg/dl)	36.3 ± 3.7	71.2 ± 9.5*
NEFA (meq/l)	0.93 ± 0.12	1.87 ± 0.35*

HOMA: Homeostatic Model Assessment; NEFA: not-esterified fatty acids. Data is presented as (mean ± SEM); *$p<0.05$.

Table III. Echocardiographic parameters of HFD mice.

	Parameters	CD (N=5)	HFD (N=6)
Gravimetric parameters	**HW/TL (mg/mm)**	6.4 ± 0.3	8.2 ± 0.4*
	LVW/TL (mg/mm)	4.1 ± 0.1	5.9 ± 0.4*
	RVW/TL (mg/mm)	0.9 ± 0.03	1.3 ± 0.07*
	Lung/TL (mg/mm)	7.9 ± 0.15	7.4 ± 0.28
Echocardiographic parameters	**SWTd (mm)**	0.88 ± 0.03	1.08 ± 0.05*
	LVEDD (mm)	3.85 ± 0.08	4.12 ± 0.08
	PWTd (mm)	0.85 ± 0.05	1.00 ± 0.03*
	SWTs (mm)	1.31 ± 0.04	1.51 ± 0.05*
	LVESD (mm)	2.30 ± 0.06	2.55 ± 0.05
	PWTs (mm)	1.26 ± 0.04	1.47 ± 0.06*
	FS (%)	39.26 ± 1.04	38.61 ± 0.99

Control diet: CD; HFD: high fat diet; HW: heart weight; LVW: left ventricular weight; RVW: right ventricular weight; TL: tibia length; SWTd: diastolic septum wall thickness; LVEDD: left ventricular end-diastolic diameter; PWTd: diastolic posterior wall thickness. Data is presented as (mean ± SEM); *$p<0.05$.

Fig. I

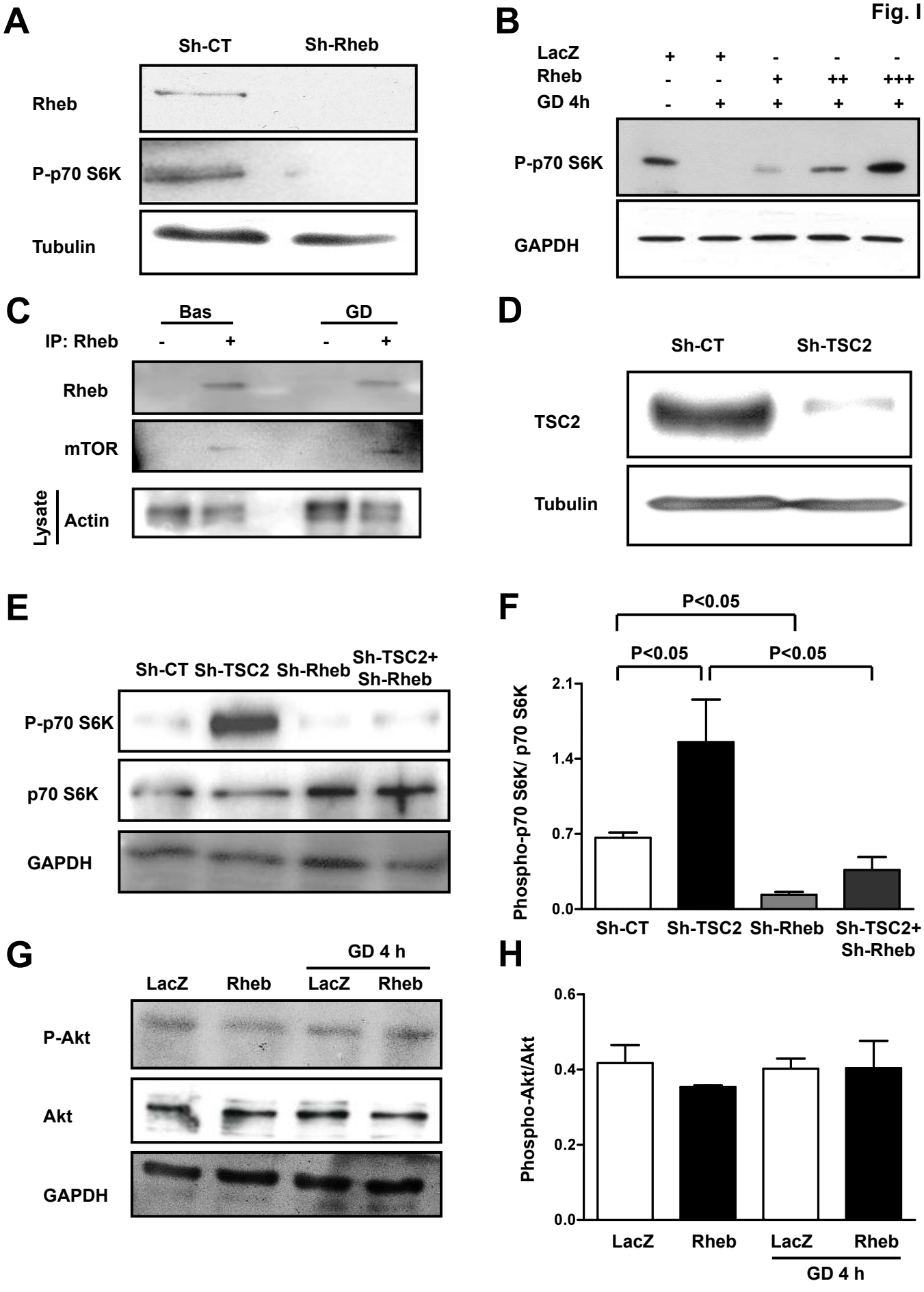

Fig. II

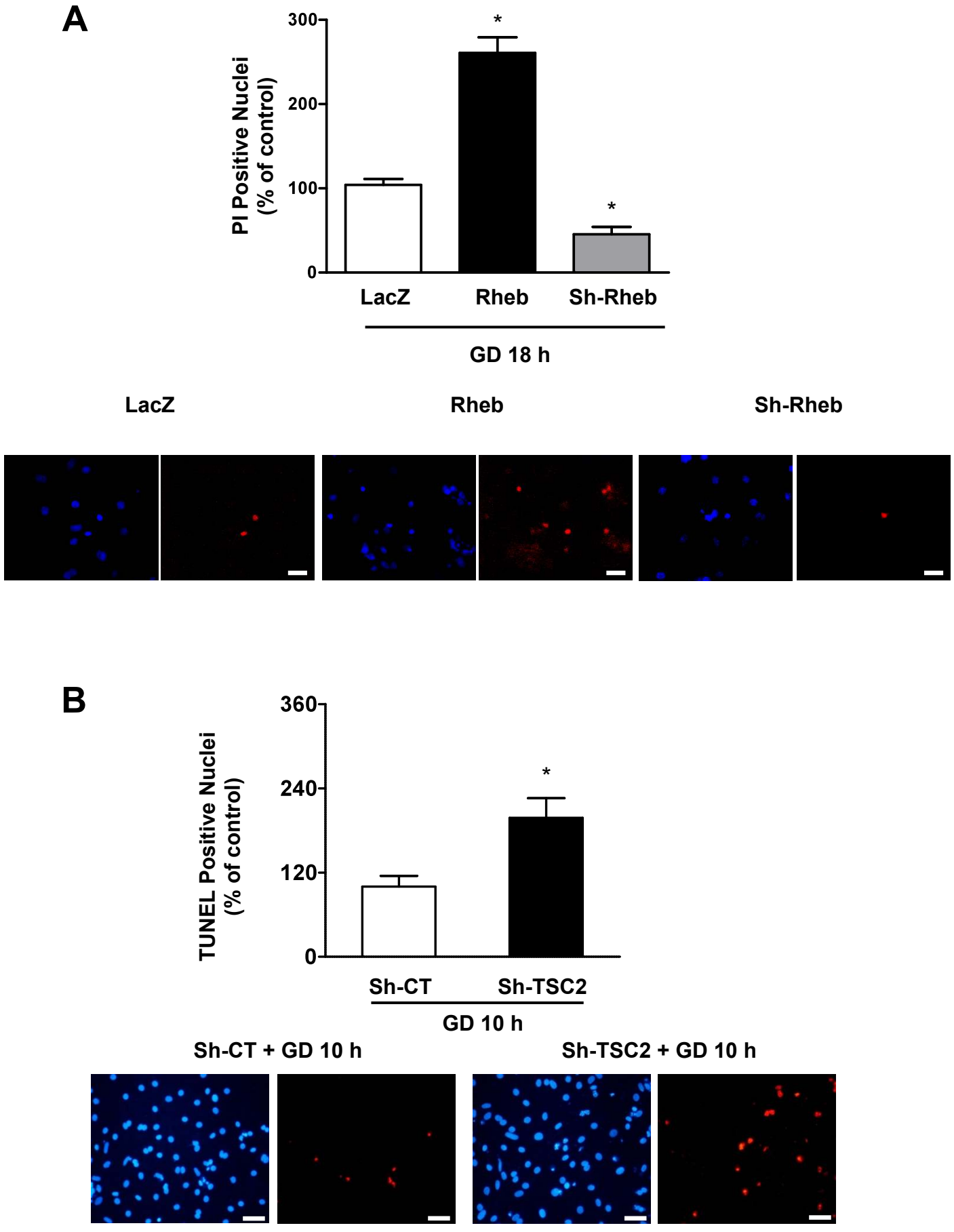

Fig. III

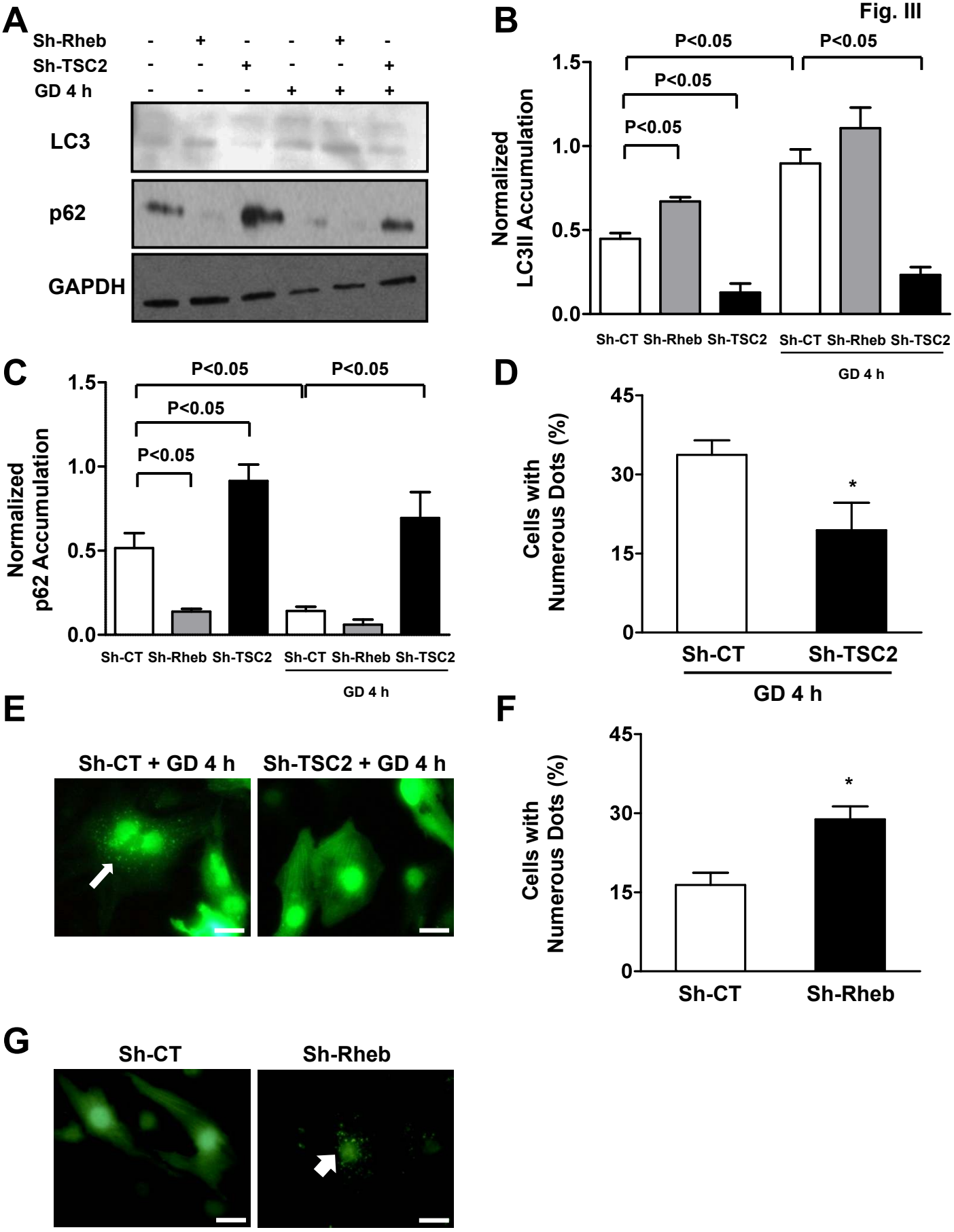

Fig. IV

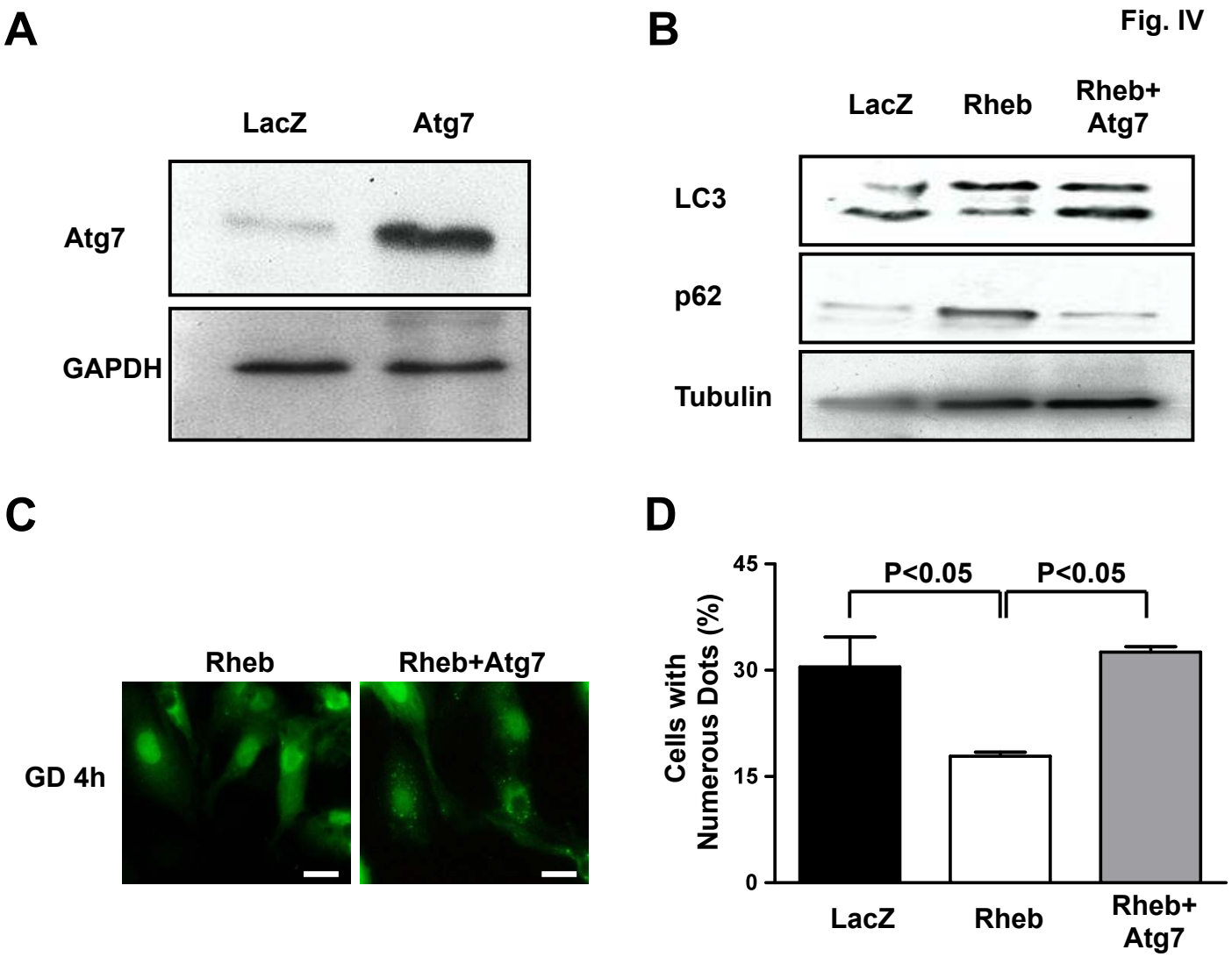

Fig. V

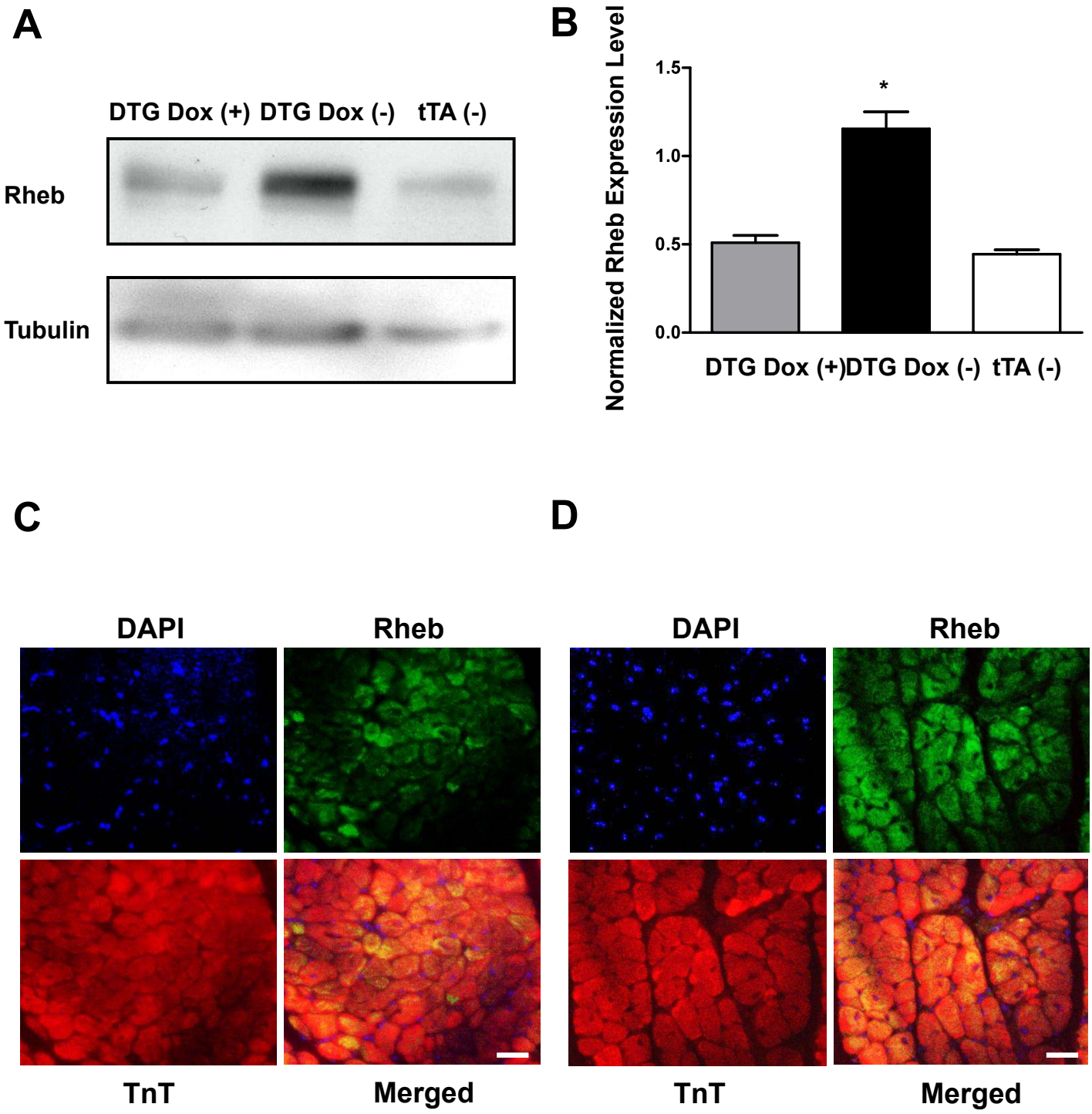

Fig. VI

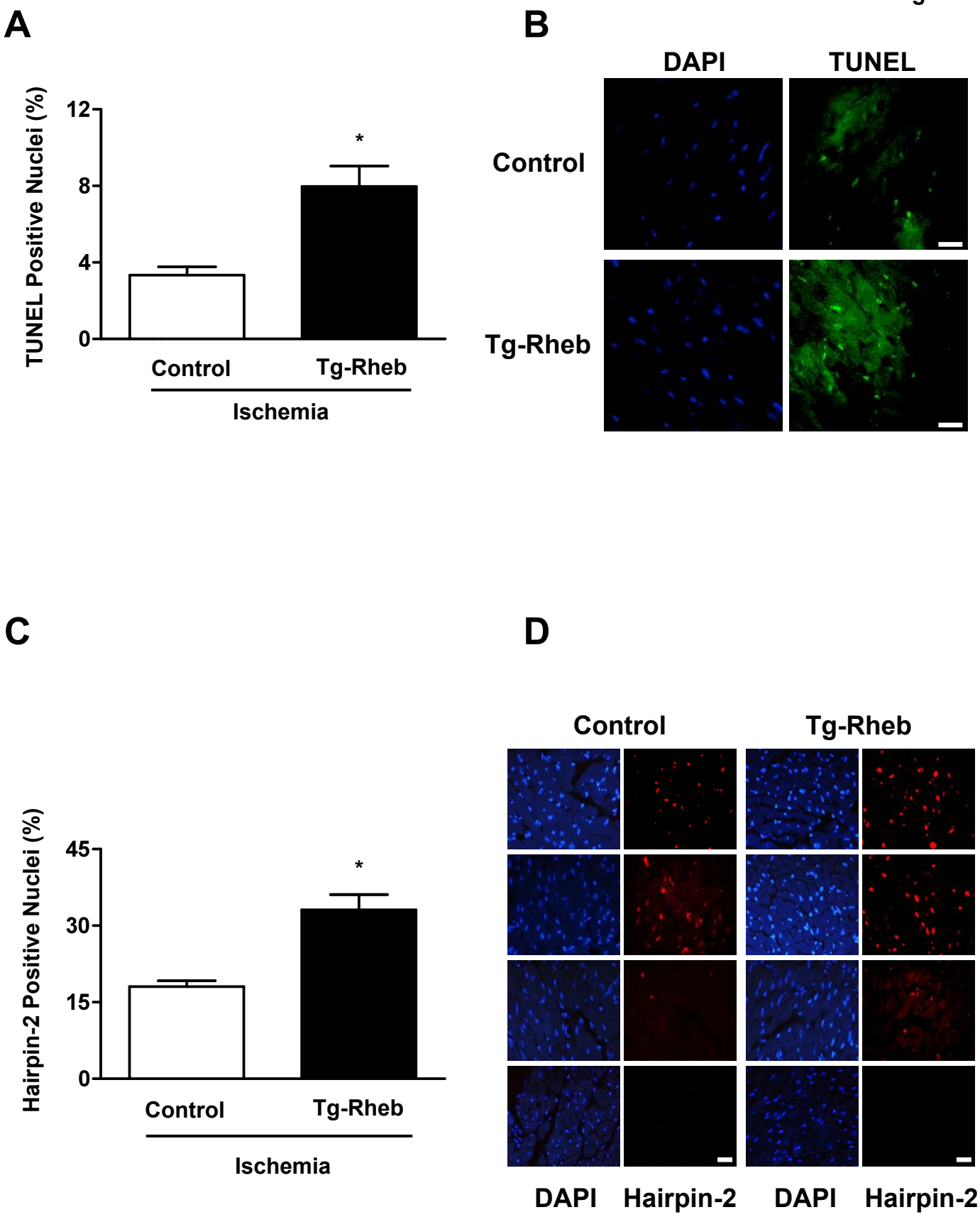

Fig. VII

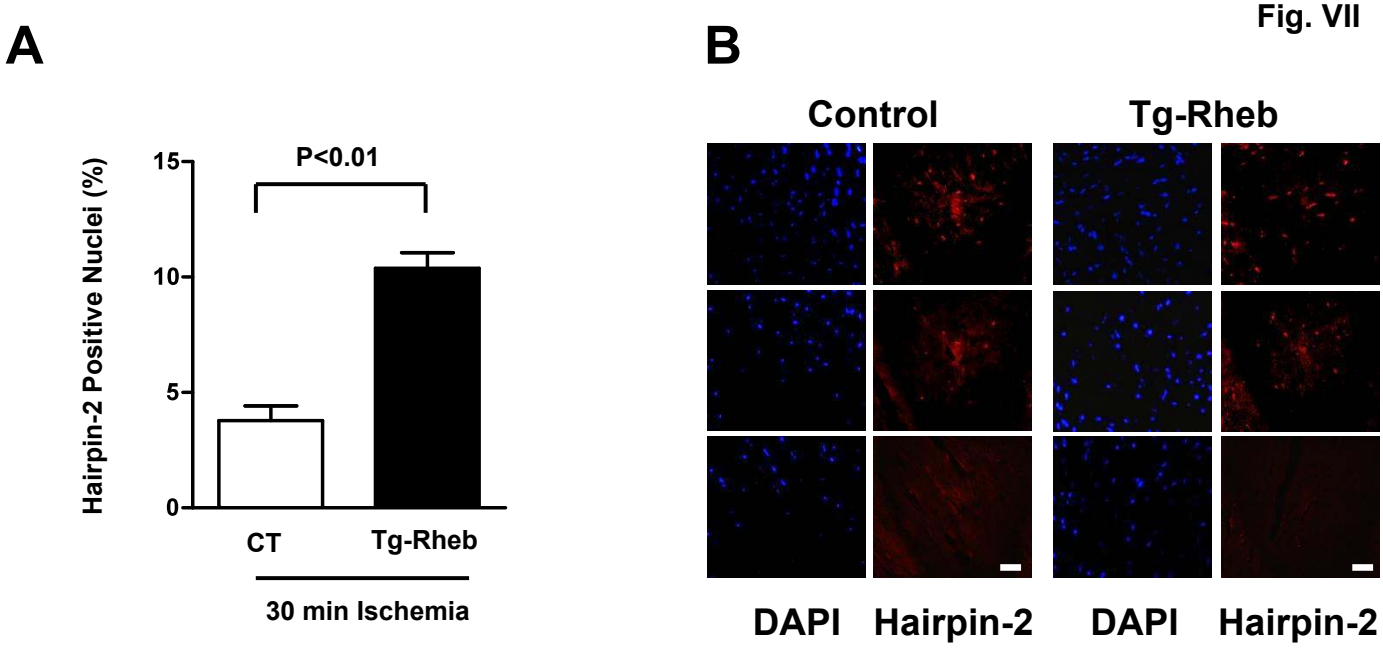

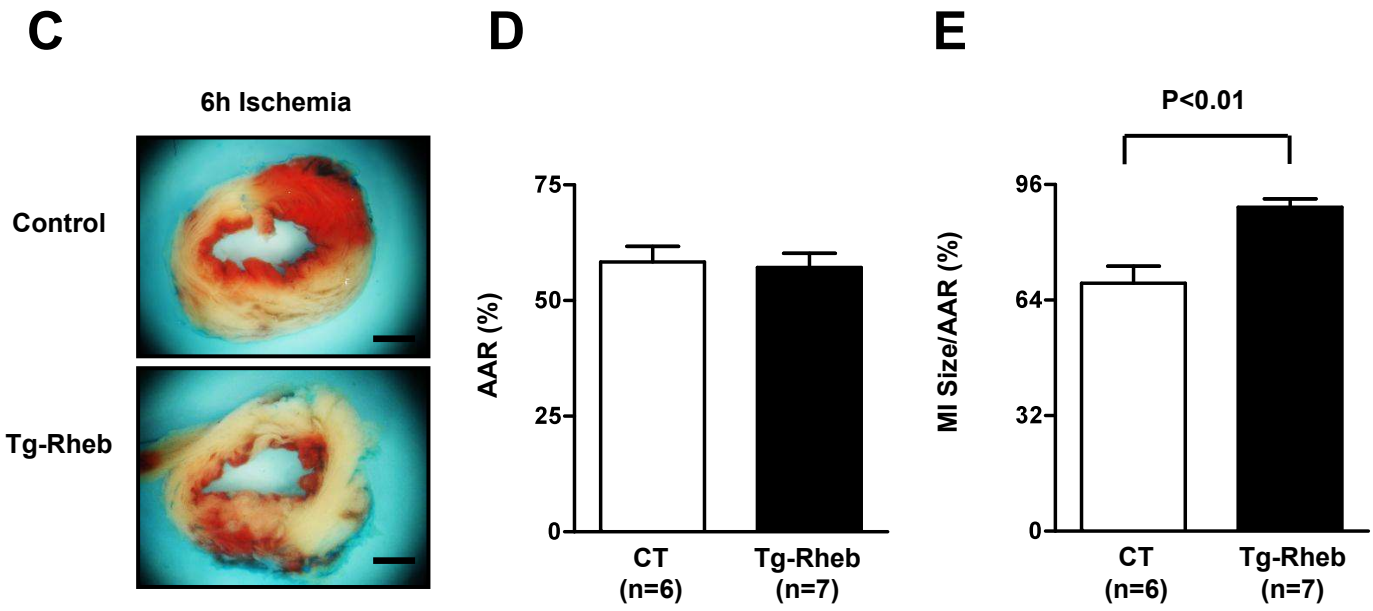

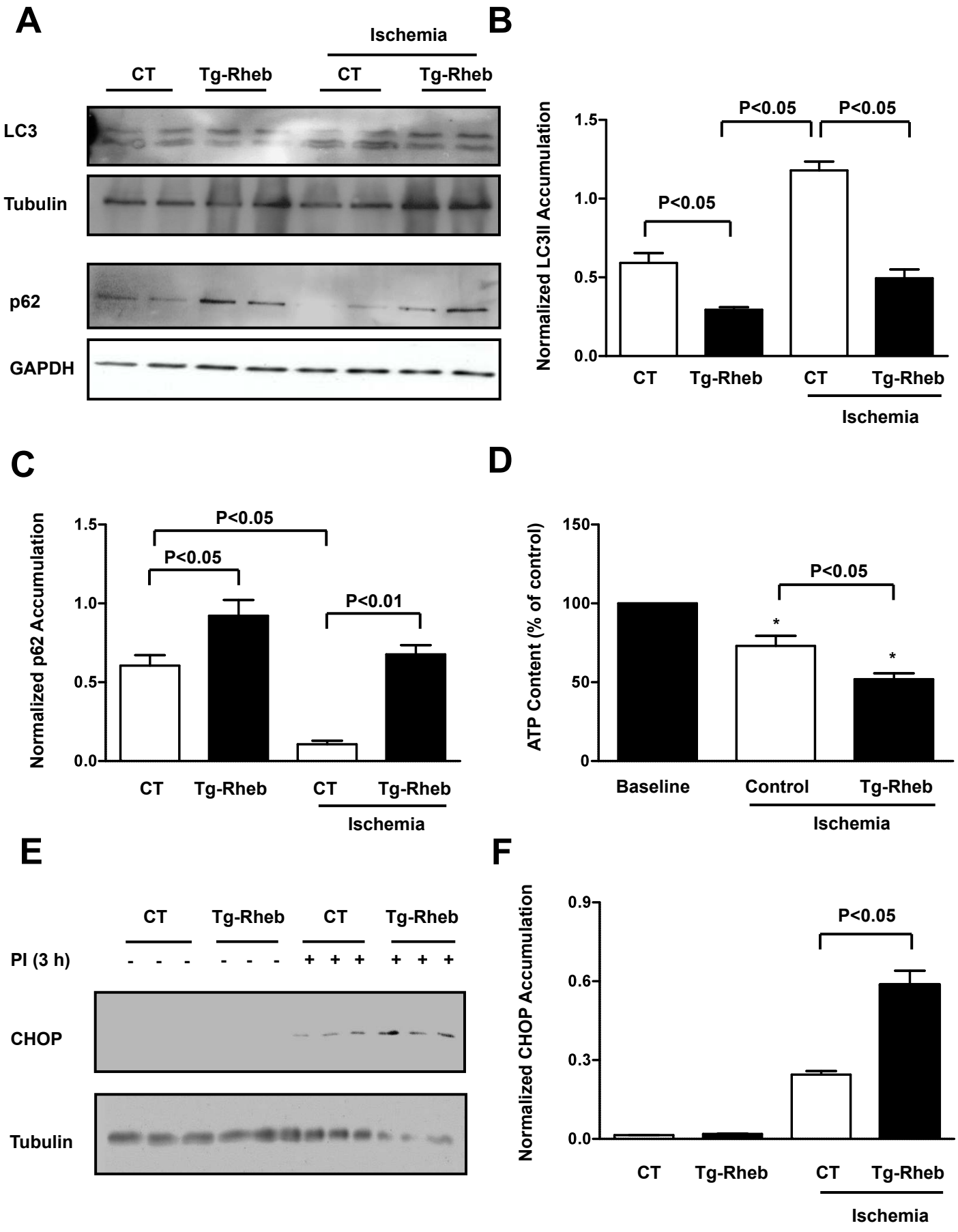

Fig. IX

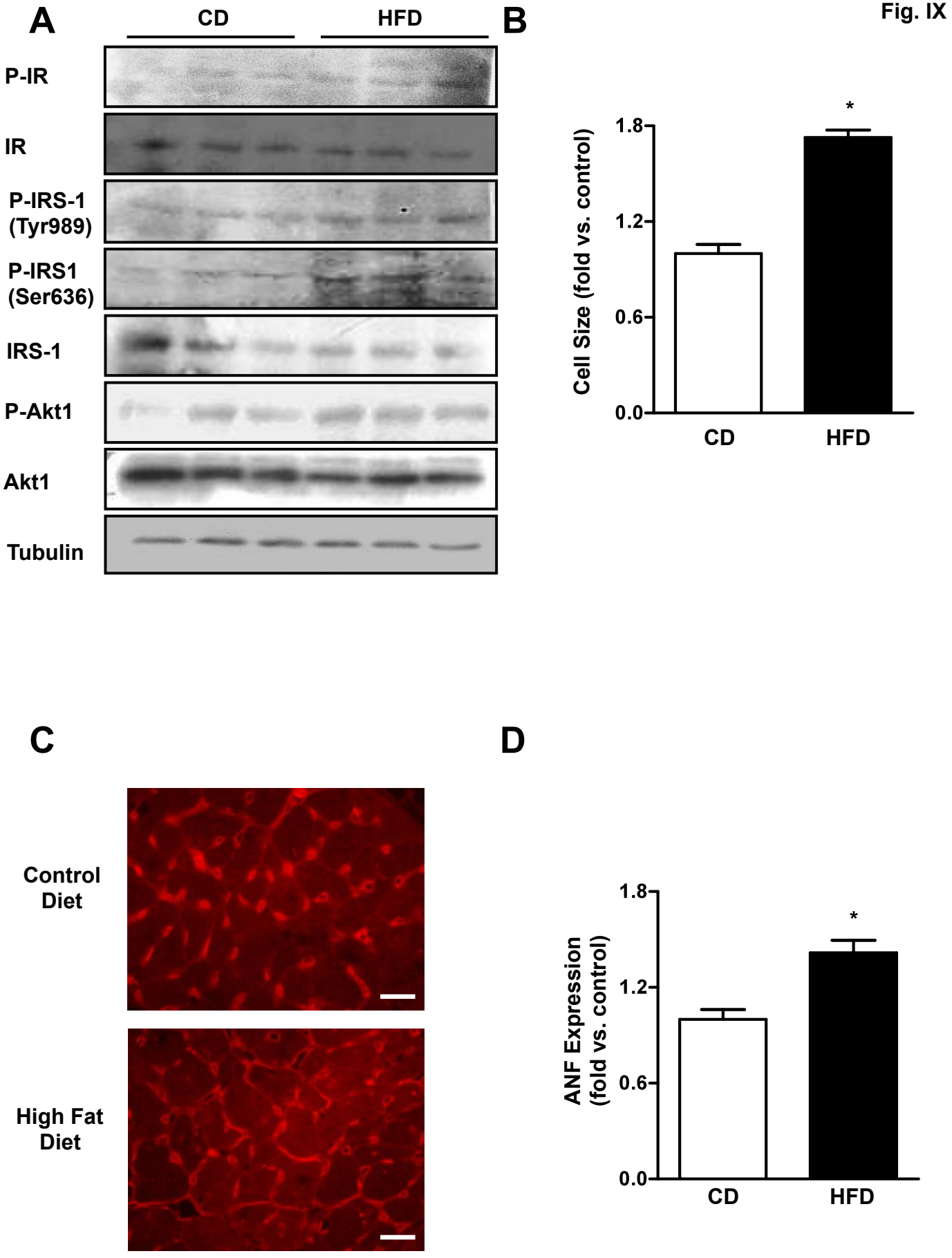

Fig. X

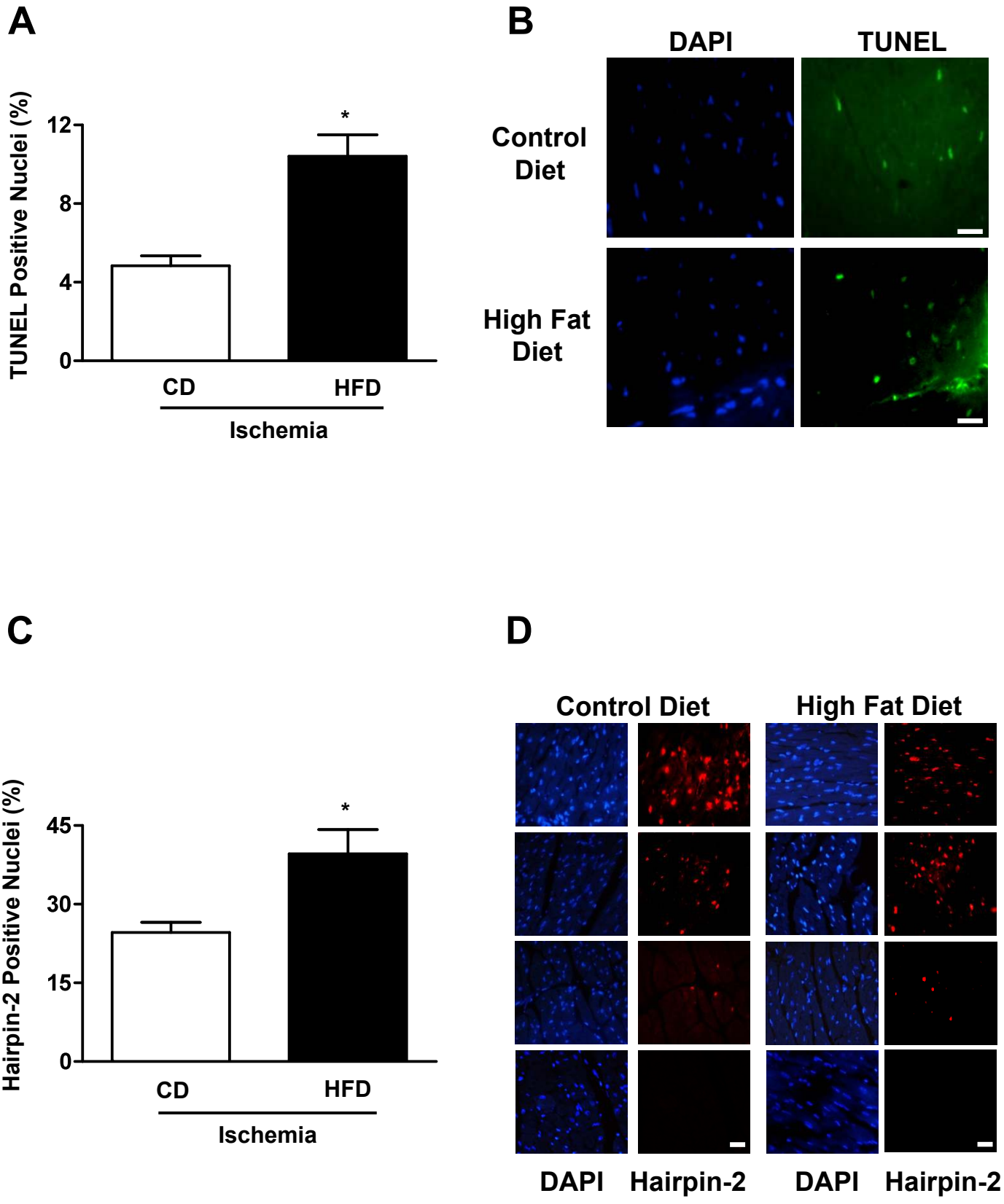

Fig. XI

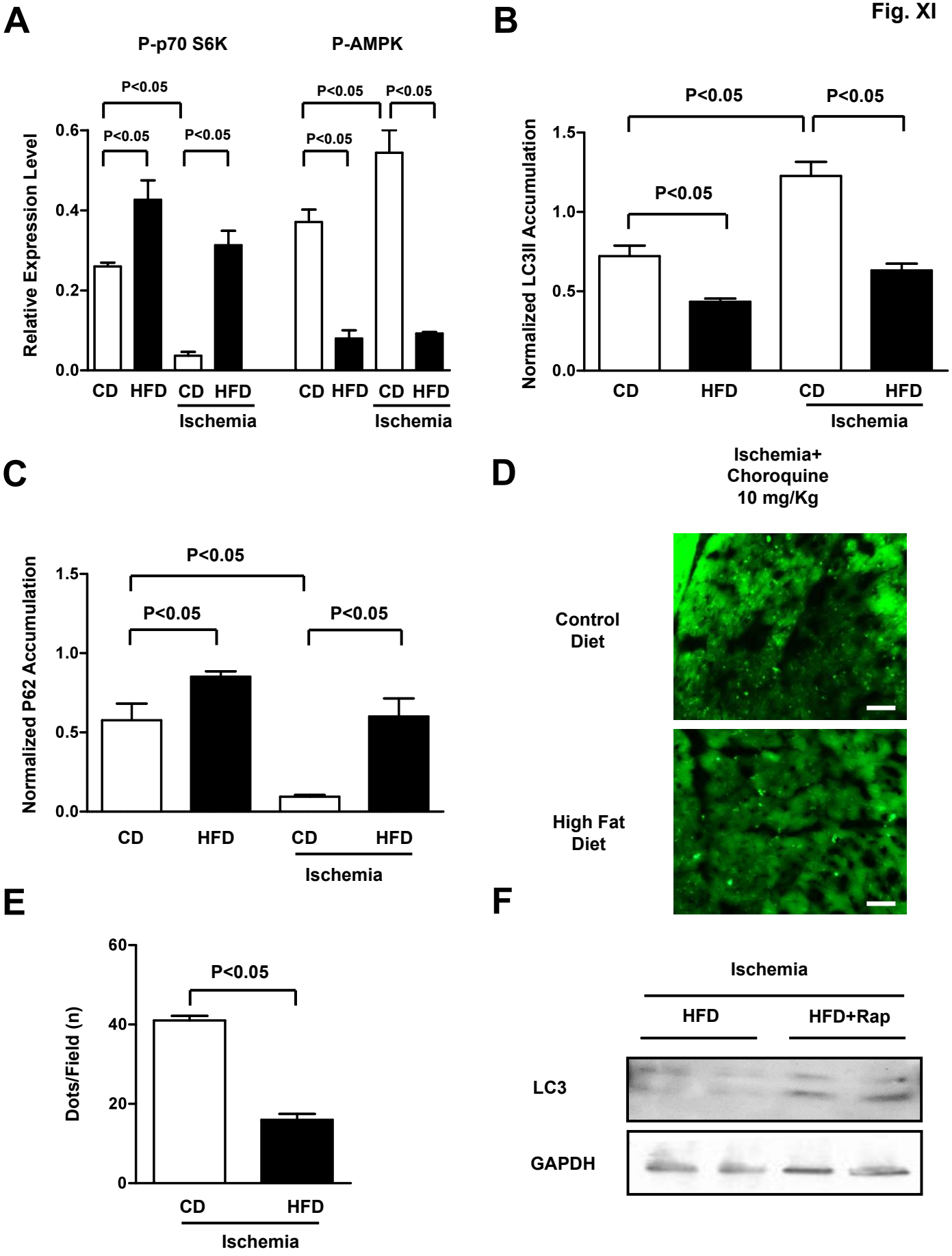

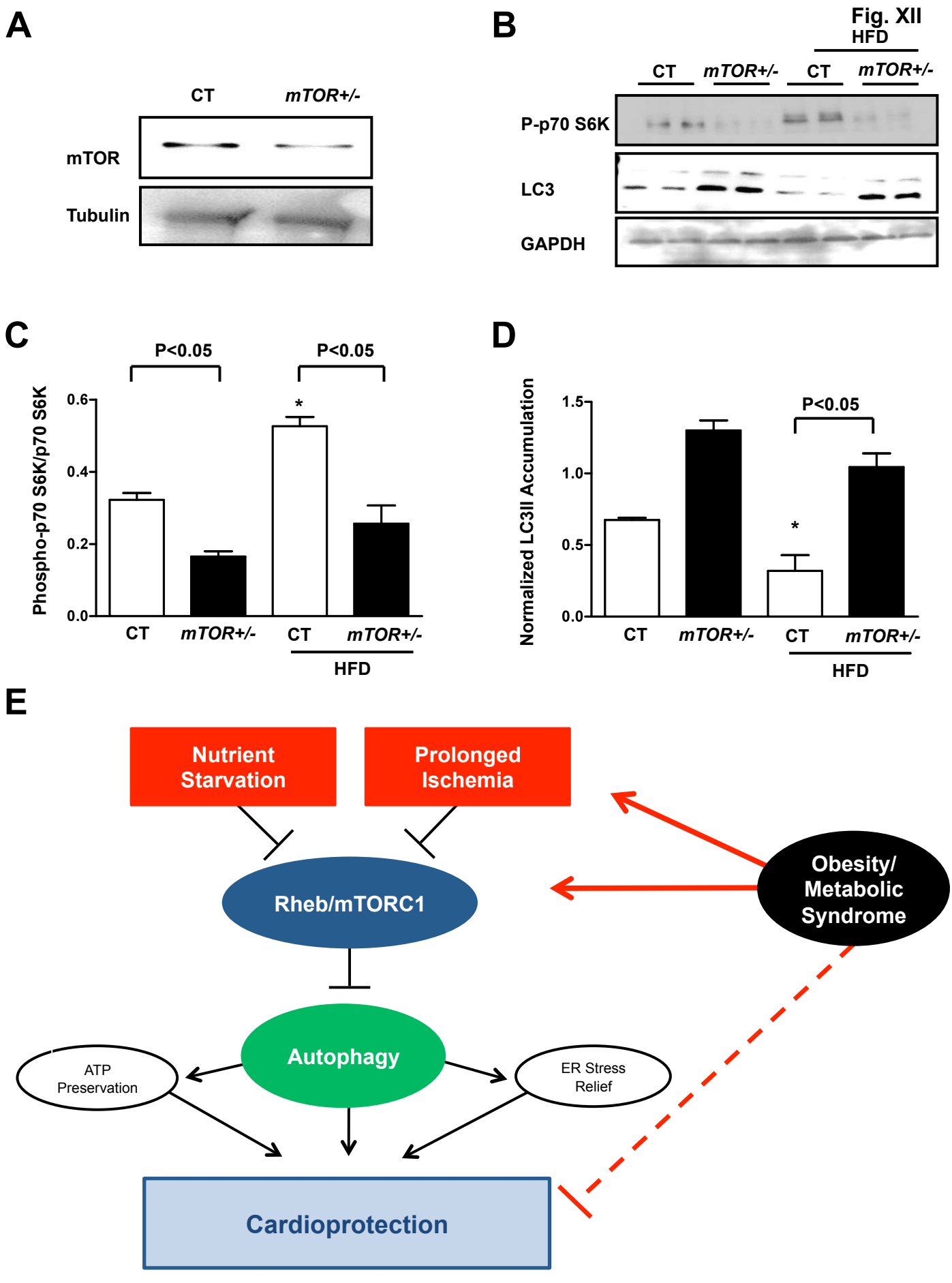
A
CT
mTOR+/-
mTOR
Tubulin
B
Fig. XII
HFD
CT
mTOR+/-
CT
mTOR+/-
P-p70 S6K
LC3
GAPDH
C
P<0.05
P<0.05
Phospho-p70 S6K/p70 S6K
0.6
0.4
0.2
0.0
*
CT
mTOR+/-
CT
mTOR+/-
HFD
D
Normalized LC3II Accumulation
1.5
1.0
0.5
0.0
P<0.05
*
CT
mTOR+/-
CT
mTOR+/-
HFD
E
Nutrient Starvation
Prolonged Ischemia
Rheb/mTORC1
Obesity/ Metabolic Syndrome
Autophagy
ATP Preservation
ER Stress Relief
Cardioprotection

Supplemental Figure Legends

Figure I. A, Rheb expression and phosphorylation status of $p70^{S6K}$ were evaluated in cardiomyocytes transduced with adenovirus expressing a short hairpin sequence, targeting Rheb for 96 hours. **B,** Phosphorylation status of $p70^{S6K}$ was evaluated in cardiomyocytes transduced with increasing doses of Ad-Rheb, after 4 hours of GD. **C,** Rheb was overexpressed in cardiomyocytes both at baseline and during GD, and it was then immunoprecipitated. Physical interaction between Rheb and mTOR was evaluated both at baseline and during glucose deprivation. **D-F,** Phosphorylation status of $p70^{S6K}$ was evaluated in cardiomyocytes with sh-TSC2 depletion, sh-Rheb, or with sh-TSC2 (D) and sh-Rheb together (E). Densitometric quantification is also shown. N=4 (F). **G-H,** mTORC2 activity, as assessed by the phosphorylation status of Akt (Ser 473), was evaluated in cardiomyocytes transduced with Ad-LacZ or Ad-Rheb, both at baseline and after 4 hours of GD. N=3.

Figure II. A, Cardiomyocytes were transduced with Ad-LacZ or Ad Rheb for 48 hours, or with sh-Rheb for 96 hours, and then subjected to GD for 18 hours. Percentage of propidium iodide-positive nuclei with respect to control cardiomyocytes was evaluated. N=3. **B,** Cardiomyocytes were transduced with sh-scramble or sh-TSC2 for 96 hours and then subjected to GD for 10 hours. TUNEL staining was performed. Data is presented as a percentage with respect to cells transduced with control adenovirus. Control bar is set at 100%. * $p<0.05$ vs. LacZ or Sh-CT. Bar=50 μm. N=3.

Figure III. A-C, Cardiomyocytes were transduced with sh-scramble, sh-TSC2 or sh-Rheb for 96 hours. LC3 isoforms and p62 accumulation were then evaluated at baseline or after 4 hours of GD. Representative immunoblots are shown (A), together with densitometric analyses of LC3-II (B) and p62 (C). N=4. **D-E,** Cardiomyocytes were coinfected with sh-scramble or sh-TSC2 for 96 hours and adenovirus expressing GFP-LC3 for the last 48 hours. After 4 hours of GD, GFP-LC3 puncta were counted. The percentage of cardiomyocytes with GFP-LC3 dots among those transduced with sh-scramble or sh-TSC2 is shown (D, * $p<0.05$), together with representative images. N=5 (E, bar=10

μm). **F-G,** Cardiomyocytes were coinfected with sh-scramble or sh-Rheb for 96 hours and adenovirus expressing GFP-LC3 for the last 48 hours. The baseline percentage of cardiomyocytes with GFP-LC3 dots among those transduced with sh-scramble or sh-Rheb is shown (F, * $p<0.05$; N=4), together with representative images (G, bar=10 μm).

Figure IV. A, Atg7 expression levels were evaluated in cardiomyocytes transduced with Ad-LacZ or Ad-Atg7. **B,** LC3-II and p62 expression levels were evaluated in cardiomyocytes transduced with Ad-LacZ, Ad-Rheb, or with Ad-Rheb together with Ad-Atg7. **C-D,** Cardiomyocytes were infected with Ad-GFP-LC3 together with Ad-LacZ or Ad-Rheb or Ad-Rheb and Ad-Atg7 together. Percentage of cardiomyocytes with GFP-LC3 puncta was evaluated during GD; bar=10 μm. N=3. **E-F,** Expression levels of LC3-II, p62, phospho-$p70^{s6k}$, Atg7 and Beclin-1 were evaluated in Ad-LacZ- and Ad-Rheb-transduced cardiomyocytes treated, or not treated, with trehalose.

Figure V. A-B, Normalized cardiac Rheb expression was evaluated in double transgenic mice ($Rheb^+$ and tTA^+; DTG) not treated with doxycycline, in DTG mice treated with doxycycline, and in $Rheb^+/tTA^-$ mice. Representative immunoblot is presented (A) with expression levels quantified (B). N=3; * $p<0.05$ vs. Dox(+) and tTA (-). **C-D,** LV myocardial tissue sections from control mice and Tg-Rheb were stained with Rheb antibody (green fluorescence) and troponin T (red fluorescence), and then counterstained with DAPI (blue fluorescence) for nuclei visualization. Representative separate and merged panels from control (C) and Tg-Rheb (D) are presented. Bar= 50 μm.

Figure VI. A-B, LV myocardial sections of Tg-Rheb and controls were subjected to TUNEL and DAPI staining. The percentage of cells that were TUNEL positive is shown. * $p<0.05$; N=3. Representative images of the staining in the border zone are shown (B, bar=50 μm). **C-D,** Tg-Rheb presented a higher necrosis rate after ischemia. LV myocardial sections were subjected to hairpin-2 and DAPI staining. The percentage of cells that were hairpin-2 positive is shown. * $p<0.05$; N=3 (C).

Representative images of the staining in the ischemic and non-ischemic areas are shown (D, bar=50 μm).

Figure VII. A-B, Tg-Rheb and control mice were subjected to 30 minutes of ischemia. The extent of myocardial necrosis was evaluated with Hapirpin 2 staining. The quantitative analysis of Hairpin 2 staining is shown in A. Representative Hairpin 2 staining is shown in B N=4. **C-E,** Tg-Rheb and control mice were subjected to 6 hours of ischemia. Representative images of the TTC staining/alcian blue staining is shown in C. Bar=50 μm. The quantitative analysis of AAR and MI size/AAR is shown in D and E, respectively.

Figure VIII. A-C, Autophagy was evaluated in Tg-Rheb at baseline and after 30 minutes or 3 hours of ischemia, as assessed by LC3-II and p62 accumulation, respectively. A representative immunoblot is presented (A), together with the densitometric analyses of LC3 (B) and p62 (C). N=4 for each group. **D,** ATP content was assessed in the ischemic area of the left ventricles after 3 hours of ischemia. Data is presented as the percentages of respective baselines. Baseline is represented as one bar arbitrarily set at 100%. * $p<0.05$ with respect to relevant baseline. N=5. **E-F,** Cardiac CHOP expression was evaluated in Tg-Rheb and controls at baseline and after 3 hours of ischemia. A representative blot is shown (E), together with the densitometric analysis; N=5 for each group (F).

Figure IX. A, Phosphorylation status of insulin receptor β (Tyr1162/3), phosphorylation of insulin receptor substrate-1 (Tyr989, Ser 636), and phosphorylation of Akt1 (Ser473) were evaluated in HFD mice and compared to control animals. **B-C,** Cell size was evaluated through WGA staining in the heart of HFD mice with respect to controls. Cell size quantification is presented as fold vs. control, which is set at 1. * $p<0.05$. In C, Representative images are also presented. N=4. Bar=50 μm. **D,** ANF expression resulted to be increased in HFD mice with respect to controls. Data is presented as fold vs. CD mice. * $p<0.05$. N=6.

Figure X. A-B, HFD mice presented a higher apoptosis rate in the ischemic area after ischemia. LV myocardial sections were subjected to TUNEL and DAPI staining. The percentage of cells that were TUNEL-positive is shown. * $p<0.05$; N=3 (A). In B, representative images of the staining in the border zone are shown. Bar=50 μm. **C-D,** HFD mice presented a higher necrosis rate after ischemia. LV myocardial sections were subjected to hairpin-2 and DAPI staining. The percentage of cells that were hairpin-2 positive is presented. * $p<0.05$; N=3. In D, Representative images of the staining in the ischemic and non-ischemic areas are shown. Bar=50 μm.

Figure XI. A, HFD mice present an increase in phosphorylation status of $p70^{S6K}$ and AMPK in the heart. Representative immunoblots are presented in Fig. 7D. N=4 for each group. **B-C,** Myocardial autophagy in obese mice was significantly inhibited compared to that in lean mice, both at baseline and after 30 minutes or 3 hours of ischemia, as indicated by LC3-II and p62 accumulation, respectively. N=4 for each group. Representative immunoblots are presented in Figure 7F. **D-E,** Chloroquine (10 mg/kg) was administered to Tg-GFP-LC3 mice fed with control diet or HFD, 4 hours before surgery. After 30 minutes of ischemia, GFP-LC3 puncta were counted in LV sections. In D, representative images are presented. Bar=50 μm. In E, quantification of the number of dots/field is shown. N=3. **F,** Rapamycin (1 mg/kg) was administered intraperitoneally to HFD and CD mice 60 minutes before coronary ligation. After 30 minutes of ischemia, autophagy was evaluated by LC3-II accumulation in the hearts of HFD mice treated with rapamycin, with respect to HFD mice treated with vehicle.

Figure XII. A, Tamoxifen (30 μg/g) was administered to α-MHC-*MerCreMer-mTOR flox/+* mice (*mTOR*+/-) and α-MHC-*MerCreMer-mTOR* +/+ mice (controls) for 7 days. Cardiac mTOR protein levels were evaluated in *mTOR*+/- and controls 3 weeks after tamoxifen administration. **B-D,** Cardiac phosphorylation status of $p70^{S6K}$, and LC3-II accumulation were evaluated in *mTOR*+/- mice and controls, fed with control diet or HFD (N=4). * $p<0.05$ vs. CT. **E,** A schematic representation of our hypothesis. Nutrient starvation and prolonged ischemia inhibit the mTORC1 pathway through Rheb

inhibition. Rheb/mTORC1 inhibition upregulates autophagy, which increases cardioprotection. On the other hand, obesity and metabolic syndrome activate the Rheb/mTORC1 pathway during prolonged ischemia, causing a defective activation of autophagy and a reduction in cardioprotection.

Supplemental References

1. Sanbe A, Gulick J, Hanks MC, Liang Q, Osinska H, Robbins J. Reengineering inducible cardiac-specific transgenesis with an attenuated myosin heavy chain promoter. *Circ Res.* 2003;92:609-616.

2. Matsui Y, Nakano N, Shao D, Gao S, Luo W, Hong C, Zhai P, Holle E, Yu X, Yabuta N, Tao W, Wagner T, Nojima H, Sadoshima J. Lats2 is a negative regulator of myocyte size in the heart. *Circ Res.* 2008;103:1309-1318.

3. Vivaldi MT, Kloner RA, Schoen FJ. Triphenyltetrazolium staining of irreversible ischemic injury following coronary artery occlusion in rats. *Am J Pathol.* 1985;121:522-530.

4. Hsu CP, Oka S, Shao D, Hariharan N, Sadoshima J. Nicotinamide phosphoribosyltransferase regulates cell survival through NAD+ synthesis in cardiac myocytes. *Circ Res.* 2009;105:481-491.

5. Didenko VV, Ngo H, Baskin DS. Early necrotic DNA degradation: presence of blunt-ended DNA breaks, 3' and 5' overhangs in apoptosis, but only 5' overhangs in early necrosis. *Am J Pathol.* 2003;162:1571-1578.

6. Guerra S, Leri A, Wang X, Finato N, Di Loreto C, Beltrami CA, Kajstura J, Anversa P. Myocyte death in the failing human heart is gender dependent. *Circ Res.* 1999;85:856-866.

7. Usui S, Maejima Y, Pain J, Hong C, Cho J, Park JY, Zablocki D, Tian B, Glass DJ, Sadoshima J. Endogenous muscle atrophy F-box mediates pressure overload-induced cardiac hypertrophy through regulation of nuclear factor-kappaB. *Circ Res.* 2011;109:161-171.

8. Matsui Y, Takagi H, Qu X, Abdellatif M, Sakoda H, Asano T, Levine B, Sadoshima J. Distinct roles of autophagy in the heart during ischemia and reperfusion: roles of AMP-activated protein kinase and Beclin 1 in mediating autophagy. *Circ Res.* 2007;100:914-922.

9. Mizushima N, Yoshimori T, Levine B. Methods in mammalian autophagy research. *Cell.* 2010;140:313-326.

10. Perry CN, Kyoi S, Hariharan N, Takagi H, Sadoshima J, Gottlieb RA. Novel methods for measuring cardiac autophagy in vivo. *Methods Enzymol.* 2009;453:325-342.

11. Inoki K, Li Y, Xu T, Guan KL. Rheb GTPase is a direct target of TSC2 GAP activity and regulates mTOR signaling. *Genes Dev.* 2003;17:1829-1834.

12. Karbowniczek M, Cash T, Cheung M, Robertson GP, Astrinidis A, Henske EP. Regulation of B-Raf kinase activity by tuberin and Rheb is mammalian target of rapamycin (mTOR)-independent. *J Biol Chem.* 2004;279:29930-29937.

13. Im E, von Lintig FC, Chen J, Zhuang S, Qui W, Chowdhury S, Worley PF, Boss GR, Pilz RB. Rheb is in a high activation state and inhibits B-Raf kinase in mammalian cells. *Oncogene.* 2002;21:6356-6365.

14. Sharma PM, Egawa K, Huang Y, Martin JL, Huvar I, Boss GR, Olefsky JM. Inhibition of phosphatidylinositol 3-kinase activity by adenovirus-mediated gene transfer and its effect on insulin action. *J Biol Chem.* 1998;273:18528-18537.

15. Scheele JS, Rhee JM, Boss GR. Determination of absolute amounts of GDP and GTP bound to Ras in mammalian cells: comparison of parental and Ras-overproducing NIH 3T3 fibroblasts. *Proc Natl Acad Sci U S A.* 1995;92:1097-1100.